Surface Enhanced Raman Spectroscopy for Environmental Analysis: Metal Sensing and Solvent Effect

by

Dongchang Yang

A thesis
presented to the University of Waterloo
in fulfillment of the
thesis requirement for the degree of
Master of Science
in
Biology

Waterloo, Ontario, Canada, 2021

Author's Declaration

I hereby declare that I am the sole author of this thesis. This is a true copy of the thesis, including any required final revisions, as accepted by my examiners.

I understand that my thesis may be made electronically available to the public.

Abstract

Raman spectroscopy is a form of molecular spectroscopy that can provide structural information on analyte molecules based on the scattering of incident light. However, Raman scattering is intrinsically weak which makes Raman spectroscopy unable to detect analytes at low concentrations. Surface-enhanced Raman Spectroscopy (SERS) can amplify the Raman signals of analytes by several orders of magnitude when the analyte adsorbs on a rough metal surface. Because of this, SERS has become a promising technique for quantitative and qualitative detection of very low concentrations of molecules in aqueous environmental samples, with both high specificity and sensitivity. With advances in nanotechnology and materials sciences, the sensitivity of this technique has been significantly improved. A variety of SERS sensors have developed and widely applied for environmental analysis, including the detection of heavy metals. Although many factors that can affect SERS detection have been investigated, a comprehensive review of this literature related to heavy metal was identified as a gap. There are many opportunities to improve SERS sensors. For example, the solvent effect on SERS detection has not been systematically studied.

This thesis comprehensively reviewed the current SERS metal sensors, with an emphasis on signal generation mechanisms, sensitivity improvement, and the quantitation challenges with real environmental samples. This review provides a systematic overview of the field and gives the insight into the current limitations and future opportunities for development of SERS metal sensors. The second component of the thesis explored how solvents with different dielectric constants alters the SERS detection. SERS detection in low dielectric constant organic solvents (*i.e.* Methylene chloride, ε=9.93) can increase the

technique's sensitivity by ~10^9-10^{10} times, allowing detection of analytes at zeptamolar concentrations. Computational modeling results were consistent with experimental observations, which supports that stronger electromagnetic enhancement of SERS substrates occurs in organic solvents through plasmon coupling. The use of this solvent effect on SERS yields fresh insights into SERS enhancement mechanisms and may facilitate additional future applications for environmental analysis.

Acknowledgements

To begin, special thanks are owed to my co-supervisors Dr. Mark Servos and Dr. Xu Zhang for giving me the opportunity to work on such an interesting and important project. Thank you for your unwavering support, patience, and valuable insight as we navigated through this project. The passion that you all have for research was very motivating. I really enjoyed learning from you about the research and life in general.

In terms of funding, I would like to thank The Natural Sciences and Engineering Research Council of Canada (NSERC) and The Canada Research Chair (CRC) program. I also want to thank Dr. Mark Servos and Dr. Xu Zhang for their financial support during the program.

I would like to thank committee members Dr. Brian Dixon and Dr. Juewen Liu for their guidance and support.

Specific to the work presented in Chapter 2 and Chapter 3, I would like to thank Brian Youden for his help on reviewing and giving advice.

I would like to acknowledge Dr. Collins Nganou for his help in Chapter 3. He helped with the theoretical computation and general advice.

I would like to extend my thanks to Dr. Ken Oakes, Dr. Andrew Carrier, David Oakley, Jane Pham, Marzieh Baneshi and Naizhen Yu for their help in the lab.

Lastly, to my parents and grandparents, thank you for your love, encouragement, and endless support.

Table of Contents

List of Figures

List of Tables

Chapter 1

General Introduction

Environmental analysis always plays an important role in environment protection, especially with the increasing concern of water pollution, including heavy metal ions and organic compounds that can represent ecosystem and human-health risks (Wei et al., 2015). In order to detect these hazardous contaminants, a wide variety of different analytical techniques and instruments has been developed. Among these, surface-enhanced Raman Spectroscopy (SERS) is a promising technique with high specificity and sensitivity, which can be used for both quantitative and qualitative research in environmental analysis. With the recent developments and incorporation of nanotechnology, SERS sensitivity has been significantly improved. In addition, SERS has the potential to be portable and rapid so that it can be utilized for on-site analysis. As a result, metal ion detection by SERS has been widely explored in past 10 years. Different methods have been developed for metal ion detection, including Hg^{2+}, Pb^{2+}, and so on, however, a comprehensive review in this emerging field is lacking.

The factors that can affect SERS detection, including different nanostructured substrates with different sizes and shapes, have been well studied (Boyack & Ru, 2009; Sabur et al., 2008) whereas the solvent effect on SERS has not been well studied. Compared to the aqueous solutions, organic solvents have lower dielectric constants that are responsible for electromagnetic wave propagation (Leung & Liu, 1990), which may affect the SERS detection sensitivity. It is hypothesized that the dielectric constants of solvents would affect

the SERS detection sensitivity, with lower dielectric constants providing higher SERS detection sensitivity.

1.1 Background to Raman Scattering

Light scattering is an optical process in which a molecule simultaneously absorbs an incident photon and emits another scattered photon (Pantell et al., 1968). If the incident and scattered photons possess the same energy levels, then the process is known as Rayleigh scattering (Young, 1981). Conversely, if the incident and scattered photons possess different energy levels it is known as Raman scattering. Raman scattering can further be classified into two categories, Stokes and Anti-stokes (Tran et al., 2019), depending on if the scattered photon gains or loses energy during the scattering process, as shown in Figure 1.1. During the Stokes process, a proportion of the energy of the incident photon is transferred to the molecule resulting in the excitation of the molecule from its vibrational ground state (v=0) to a higher vibrational state (v=1). Consequently, the energy of scattered photon (E_{Sca}) is smaller than the energy of the incident photon. The Anti-stokes is the contrary process where the molecule is relaxed from a higher vibrational state to the vibrational ground state and transferred those energy to the scattered photon which results in the higher energy of the scattered photon (E_{Sca}) than the incident photon (E_{Inc}).

However, compared to the Stokes process, the Anti-stokes process is less common since the molecule must already be at a higher vibrational state before the scattering process, which only occurs under the certain condition such as through the thermal excitation (Ru & Etchegoin, 2008).

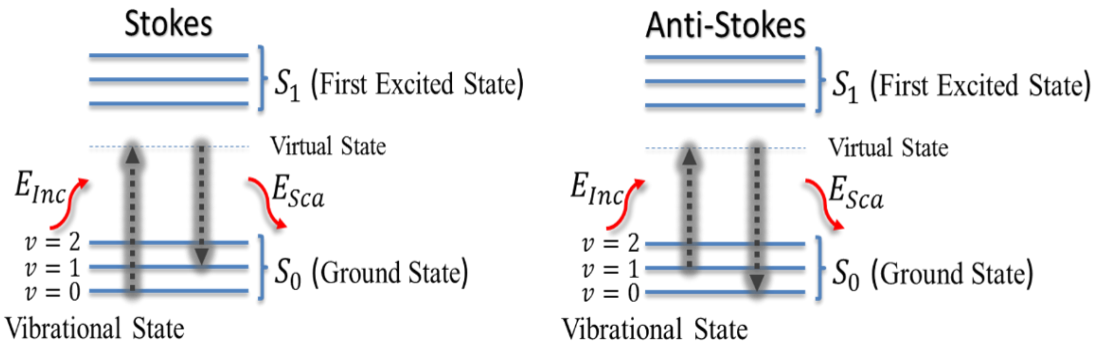

Figure 1.1 Schematic of Stokes process and Anti-stokes process caused Raman scattering, where E_{Inc} and E_{Sca} represents energy of incident photon and scattered photon, respectively. Adapted from Ru and Etchegoin (2008).

1.2 Raman Spectroscopy

In analytical science, Raman spectroscopy is a technique utilized for molecule identification. In Raman spectroscopy, samples are radiated with a laser of certain wavelength, and the scattered light is collected by the detector. In a typical Raman spectrum (Figure 1.2), intensity is always presented as a function of Raman shift which represents the energy difference between the scattered light and the incident light caused by the Stokes process ($\Delta E = E_{Inc} - E_{Sca}$). Therefore, theoretically, for any analyte, Raman spectrum can provide its specific vibrational structure. Compared to Gas chromatography–mass spectrometry, Raman spectroscopy is far simpler, more cost effective, and does not result in the destruction of the sample.

However, Raman scattering is intrinsically weak as only a tiny proportion of incident light can be scattered by molecules compared to other optical processes such as absorption and transmission. This is especially true for analytes at low concentrations (<μM) or for molecules have small Raman cross-section (the effective area in a molecule that able to

scatter the incident light) resulting in an inability to distinguish the Raman signals from the spectrum background noise (Ru & Etchegoin, 2008). Because of this Raman spectroscopy has a limited detection sensitivity, preventing Raman spectroscopy from being an ultrasensitive analytical tool. For example, in environmental analysis Raman spectroscopy is not viable for real-time monitoring due to the extremely low concentrations of the target pollutants (Halvorson & Vikesland, 2010).

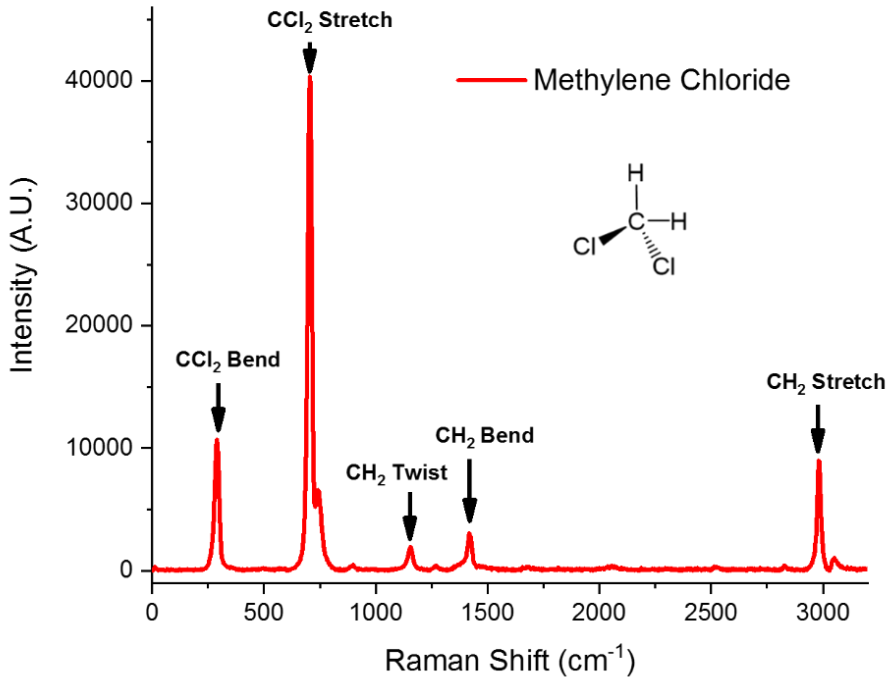

Figure 1.2 Typical Raman spectrum of methylene chloride.

1.3 Surface Enhanced Raman Spectroscopy (SERS)

SERS refers to the amplification of a molecule's Raman signals following absorption onto a metal or rough surface. This phenomenon was first observed by Fleischmann and his co-workers in 1974 (Fleischmann et al., 1974), where pyridine adsorbed on a roughened silver electrode showed greater than expected Raman signals. Since the discovery of this

enhancement phenomenon, SERS has attracted researchers' interest both for its mechanism and for its potential applications (Schatz et al., 2006; Tian, 2005; Liu et al., 2007). With the rapid development of nanotechnology, metal nanoparticles, due to their unique optical properties, have been employed as SERS substrates to replace the traditional metal electrodes. This significantly improves the sensitivity and reproducibility of SERS measurements (Sharma et al., 2012). Over the last decade of research, two independent enhancement mechanisms have been proposed to account for the signal enhancement, which are electromagnetic enhancement and chemical enhancement. Because of the enhanced sensitivity, SERS has been applied to a diverse range of analytical fields, including chemical detection, environmental monitoring, and biological sensing (Halvorson & Vikesland, 2010).

1.4 SERS Limit of Detection (LOD)

Single molecule detection (SM) was first reported by Nie and Emory in 1997 (Nie & Emory, 1997), where single rhodamine 6G molecules were probed by SERS. The reported enhancement factors (EFs) of SM-SERS were achieved on the order of 10^{14} to 10^{15}. However, this ultra-high detection sensitivity could only be achieved when the single molecules were located on hotspots within the volume of excitation beam. The hot spots refer to the high-curvature regions on the nanoparticle surface or the nanogap (<10 nm) between adjacent nanoparticles; they are the locations from where the analyte molecule can experience the strongest electromagnetic field enhancement. In addition, the volume of excitation beam, also known as sampling area, is small when compared to the sample volume. Therefore, in fact, the LOD of SM-SERS is on the level of nM (10^{-9} M) or pM (10^{-12} M) which limits its applicability for on-site environmental analysis and analytical chemistry.

1.5 Research Objectives

This thesis explores two aspects of SERS used for environmental analysis. The first is a literature review of SERS principals and applications for metal ion detection and the second is an experimental examination of the solvent effect on SERS detection. The specific objectives of the thesis were to:

1. Comprehensively review the field of the metal ion detection using SERS
2. Investigate the effect of organic solvent on SERS detection and development of a method where SERS measurement can be conducted in organic solvents.

In Chapter 2, the current methods developed for different metal ion detection have been comprehensively reviewed including the signal generation mechanism, sensitivity, and quantitative analysis of SERS metal sensors. Additionally, the gap between the current research and the application to real environmental analysis has been identified. In Chapter 3, the solvent effect on SERS detection is explored by examining the SERS sensitivity in organic solvents with different dielectric constants. Both experimental evidence and theoretical computation are provided.

Chapter 2

Metal Sensing by Surface Enhanced Raman Spectroscopy

2.1 Introduction

Heavy metal pollution in aquatic environments has drawn wide attention and is a serious concern globally (Vardhan et al., 2019; Zhou et al., 2008). The fate and transport of heavy metals in the environment is complex as they can undergo many processes including dissolution, precipitation, sorption, and complexation (Li et al., 2014). Heavy metals, such as As, Cd, Pb, Hg can be toxic to humans and other species at low concentrations and represent a considerable environmental risk (Arjomandi & Shirkhanloo, 2019; Duruibe et al., 2007; Tchounwou et al., 2012). Analytical techniques with high sensitivity towards metal ions are needed to support environmental detection, monitoring and remedial actions (Vareda et al., 2019; Wuana et al., 2011).

Current well-established analytical techniques for the detection of metal ions include atomic absorption spectroscopy (AAS), atomic fluorescence spectrometry (AFS), cold vapor atomic absorption spectrometry (CVAAS), cold vapor atomic fluorescence spectrometry (CA-AFS) (Canário et al., 2004), and inductively coupled plasma-mass spectrometry (ICP-MS) (Liu et al., 2011). All of these techniques provide accurate and sensitive detection of metal ions, however, expensive instruments, sophisticated sample preparation, and time-consuming operation make these techniques difficult for portable and on-site environmental analysis. The development of simple, rapid, and cost-effective techniques for metal ion detection is highly desirable. Surface-Enhanced Raman Spectroscopy (SERS) is a promising

analytical tool with high sensitivity and specificity, which can detect as little as a single molecule while also providing structural information (Kneipp et al., 2008; Moskovits et al., 2007). Because of its high sensitivity and selectivity, SERS has been widely explored for applications such as environmental monitoring and biological imaging (Ong et al., 2020).

The rapid development of nanotechnology has advanced SERS technology greatly and has enabled it to be a considered as an approach for more rapid and sensitive sensing applications (Mosier, 2017). Although detection by SERS sensors for metal ions, such as Hg^{2+} and As^{3+}, has been reviewed previously (Hao et al., 2015; Song et al., 2016; Sun et al., 2016), the focus of these reviews has been on specific metals rather than a comprehensive overview. SERS metal sensors have also been mentioned in some related reviews where comparisons with other types of sensors, such as colorimetric, fluorescence and electrochemical based metal sensing have been made (Ding et al., 2016; Yang et al., 2017). Recently, several reviews have included inorganic ion detection by SERS sensors (Ji et al., 2021) but there is no comprehensive review available for atomic metal ion sensing by SERS. This current review addresses this gap by first examining the mechanisms of how SERS signals are generated, upon the interaction between the target metal ions and the sensor system (signal generation mechanism), then discussing sensitivity improvement of the SERS metal sensors depending on the different signal generation mechanisms, and quantitative analysis for SERS detection of metal ions in environmental applications.

2.2 Enhancement Mechanisms of SERS

2.2.1 Raman Spectroscopy and SERS

Raman spectroscopy is a technique that is utilized for molecule identification, including the structural information and vibrational modes (Lyon et al., 1998). In Raman spectroscopy, samples are irradiated with a laser of a certain wavelength and the scattered light is collected by a detector, providing the Raman spectra of analyte molecules. However, Raman scattering is intrinsically weak, wherein only ~1 out of 10^4 photons is effectively scattered (Smith & Dent, 2019). Surface-Enhanced Raman Spectroscopy (SERS) refers to the amplification of a molecule's Raman signals by several orders of magnitude when the molecules of interest are adsorbed on or close enough to a rough, noble metal surface. Due to their excellent optical properties, noble metal nanoparticles such as gold nanoparticles (AuNPs), silver nanoparticles (AgNPs), and copper nanoparticles (CuNPs) have been extensively employed as a substrate to improve SERS sensitivity (Ru & Etchegoin, 2009). The Raman signal enhancement is mainly considered to be a result from electromagnetic enhancement and chemical enhancement, where the electromagnetic enhancement is based on the nanoparticle's localized surface plasmon resonance and dominates the signal enhancement (Schatz et al., 2006).

2.2.2 Electromagnetic Enhancement

Electromagnetic enhancement, within the context of SERS, refers to the enhanced local electromagnetic field coupled by both the incident light and surface plasmon oscillation. When incident photons interact with a metal surface, conduction electrons on the metal

surface are excited to collectively oscillate (Figure 2.1), which is known as a surface plasmon excitation. Surface plasmon can either propagate at the interface of the metal and the medium or be localized on metal nanoparticles surface (Schatz et al., 2006). When the frequency of the electrons collective oscillation is equal to the frequency of incident photons, the effect is termed Surface Plasmon Resonance (SPR). For nanoparticles, the effect is more specifically known as a Localized Surface Plasmon Resonance (LSPR) as the coherent electron oscillation (*i.e.,* the plasmon quasiparticle) is limited to the discrete metal nanoparticle surface and cannot be propagated between discrete metal nanoparticles. When a LSPR occurs, an extra electromagnetic field is generated. For analytes absorbed on the surface of a nanomaterial, they can experience an enhanced local electromagnetic field generated by the coupling of the incident light and the electromagnetic field generated by the LSPR, resulting in a significant Raman signal enhancement (Schatz et al., 2006). However, some experimental observations cannot be solely by electromagnetic enhancement. To further explain the SERS phenomena, a second enhancement mechanism that operates independently of the electromagnetic enhancement mechanism has been proposed and supported, which is known chemical enhancement. To benefit enhancement from the chemical mechanism, molecules need to be chemisorbed onto the metal surface.

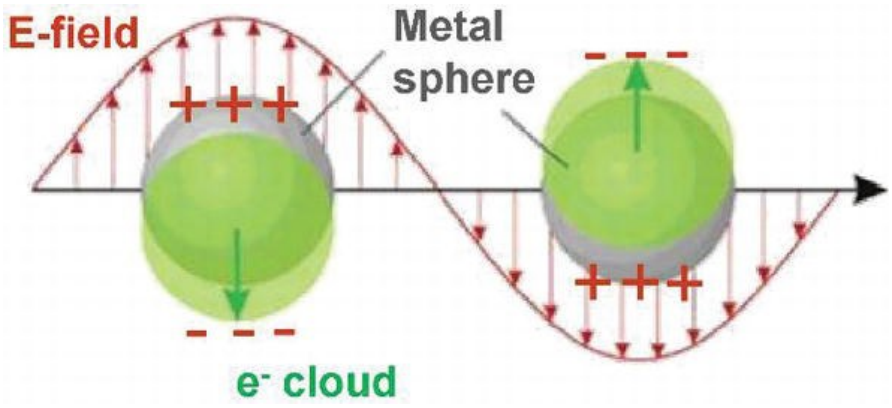

Figure 2.1 Electromagnetic enhancement generated by metal nanoparticles, where E represents the electromagnetic filed of incident light while e^- represents the conduction electrons on the metal surface. Adopted from El-Said et al., (2017).

2.2.3 Chemical Enhancement

Chemical enhancement is classified into two mechanisms depending on whether the metal acts as an intermedium or not (Doering & Nie, 2002). When the analyte molecule is chemisorbed on the metal surface, the wavefunctions of the metal and the molecule are overlap, resulting in a renormalization of their molecular orbitals. After renormalization, if the energy of incident light is high enough to directly excite the electron from the renormalized the highest occupied molecular orbital (HOMO) to the lowest unoccupied molecular orbital (LUMO), the mechanism is known as resonant chemical enhancement. Alternatively, if the energy of an incident photon is not able to excite the electrons of the adsorbate from HOMO to LUMO, a charge transfer mechanism can also occur. Here, the electron is transferred first from the HOMO to an intermediate level within the metal nanoparticle, and then further transferred to the LUMO (Doering & Nie, 2002).

2.2.4 Hot Spot Theory

A crucial concept in SERS technology is the generation of a “hot spot” which represents the location where the adsorbed molecule can experience the strongest electromagnetic field. The hot spot usually occurs at a sharp tip or high curvature region of the nanoparticle, such as in silver nano-prisms (Ru et al., 2008). The hot spot can also be generated in the gap between two neighboring nanoparticles. When two individual nanoparticles are excited by incident light and the surface plasmon resonance is generated, if these two nanoparticles are close, there will be a plasmon-plasmon coupling in the nanoparticle gap which induces an enhanced electromagnetic field in the interacting nanogap. Usually, this hot spot generation mechanism is effective when the nanogap between two neighboring nanoparticles is less than 10 nm (Ru et al., 2008). The two different hot spot types are illustrated in Figure 2.2.

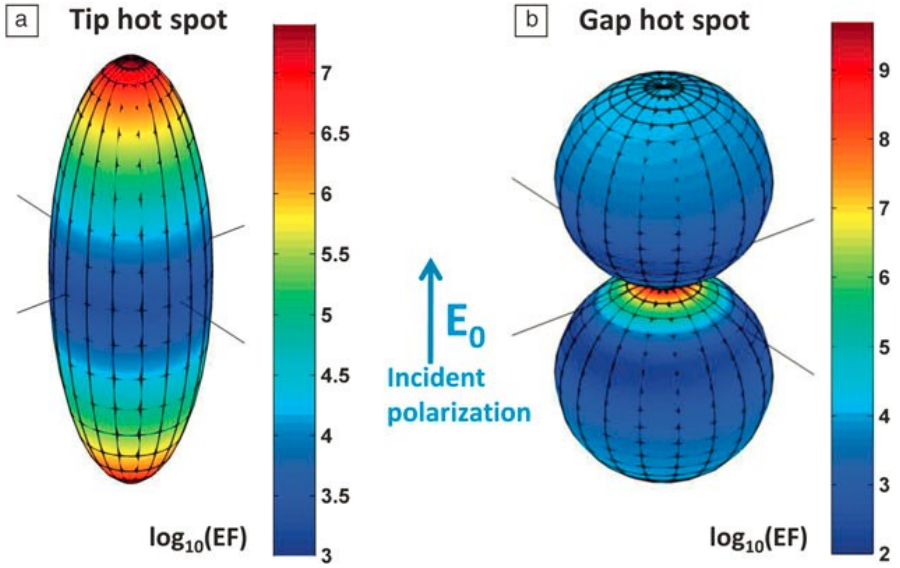

Figure 2.2 Electromagnetic hot spot in nanostructures. Adopted from Ru and Etchegoin (2012).

2.3 Signal Generation Mechanism of SERS Metal Sensors

SERS is a form of molecular spectroscopy that is well known for its label-free detection. However, metal ions lack the vibrational modes of larger molecules and have a negligible Raman cross-section, which making it impossible to directly detect the SERS signals of metal ions. Therefore, indirect SERS measurements using a labeled Raman reporter molecule is employed for metal sensing. Generally, the labeled reporter molecules exhibit the following features: first, the reporter molecule should have a relatively large Raman cross-section; second, under the laser excitation, the polarizability of the molecule can be changed and has distinct spectral features with sharp and narrow peaks observable (Pérez-Jiménez et al., 2020). By monitoring the alteration of the spectrum features of the reporter molecule when the target metal ions interact with the SERS sensor (*e.g.,* the new peak formation, the peak position shift, the peak intensity change) the detection of metal ions can be achieved.

An effective SERS sensor for metal ions detection should include three components:

1. an active substrate, which could generate an enhanced SERS field under laser excitation;
2. a capture agent for recognition and selectivity, with a high affinity towards the target metal ions;
3. a Raman reporter molecule that is used to generate the spectroscopic signal and confirm the exitance of the target metal ions.

In the presence of metal ions, these three components of the SERS sensor can behave and respond differently, thus causing the spectroscopic alteration of the reporter molecule. Essentially, metal ions can either directly interact with the reporter molecule adsorbed on the

SERS substrate surface or interact with a capturing agent which can indirectly affect the reporter molecule or the SERS substrate. Depending on the responses of the SERS sensor upon the interaction with metal ions, the signal generation mechanisms can be divided into four categories (as shown in Figure 2.3):

1. reporter molecular recognition;
2. inter-substrate distance change;
3. reporter molecule location change;
4. substrate property/concentration change.

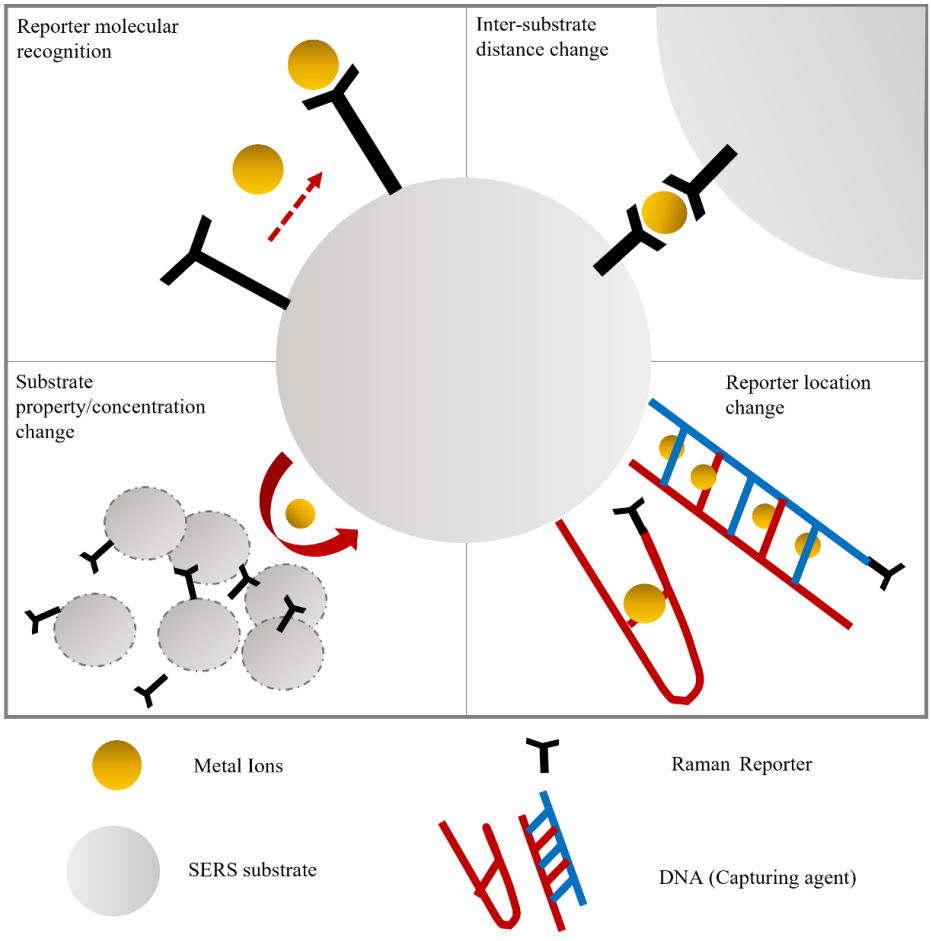

Figure 2.3 Overview of the signal generation mechanism of SERS metal sensors. Four signal generation mechanisms, which are reporter molecular recognition (top left), inter-substrate distance change (top right), substrate property/concentration change (bottom left), reporter location change (bottom right).

2.3.1 Reporter Molecular Recognition

SERS is a typical molecular spectroscopy approach that can give structural information of the molecule adsorbed on the substrate surface. Therefore, metal ions can be detected by monitoring changes to the reporter SERS spectrum upon the direct interaction between the reporter molecule and the target metal ions (Figure 2.3). In this mechanism, the reporter molecule, usually an organic ligand capable of forming a metal-complex, adsorbs on the substrate surface and acts both as a capturing agent and a SERS signal reporter. Upon the interaction with target metal ions, the reporter molecule may experience displacement from the substrate, orientation and/or structure changes on the substrate surface. If the reporter molecule displaces from the substrate surface, it will usually cause a "turn-off" of the SERS signal of the reporter molecule. However, if the interaction between metal ions and the reporter molecule alters the orientation and/or the structure change, the electron density and the vibrational modes of the reporter molecules will be dramatically changed. This results in the distinguishing spectral features compared to the original SERS spectrum of the reporter molecule, involving a characteristic peak shifting, new peak generating, or peak intensity change in the spectra region. Figure 2.4 summarizes several examples of how metal ions can be detected using a variety of reporter molecular recognition systems. The adsorbed reporter molecules can be displaced from the substrate surface when the target metal ions have higher affinity towards the reporter molecules than the nanoparticle surface. Therefore, with the

decreasing surface coverage of reporter molecules on the surface, a "turn-off" of the SERS signals can be observed. For example, as shown in Figure 2.4A, a popcorn shaped Au nanomaterial was capped and protected by tryptophan (Senapati et al., 2011). In the presence of Hg^{2+}, a tryptophan-Hg complex could be formed because of the higher binding constant, resulting in the release of tryptophan from the substrate surface. In addition, with the loss of protection of tryptophan, the popcorn shaped Au nanomaterial dissolved its sharp edge, resulting in the decreasing SERS activity (Senapati et al., 2011). Similarly, cucurbit[7]uril (CB[7]) pre-adsorbed on Au and graphene constructed SERS substrate surfaces and also undergo specific displacement upon the interaction with Pb^{2+} (Shi et al., 2016).

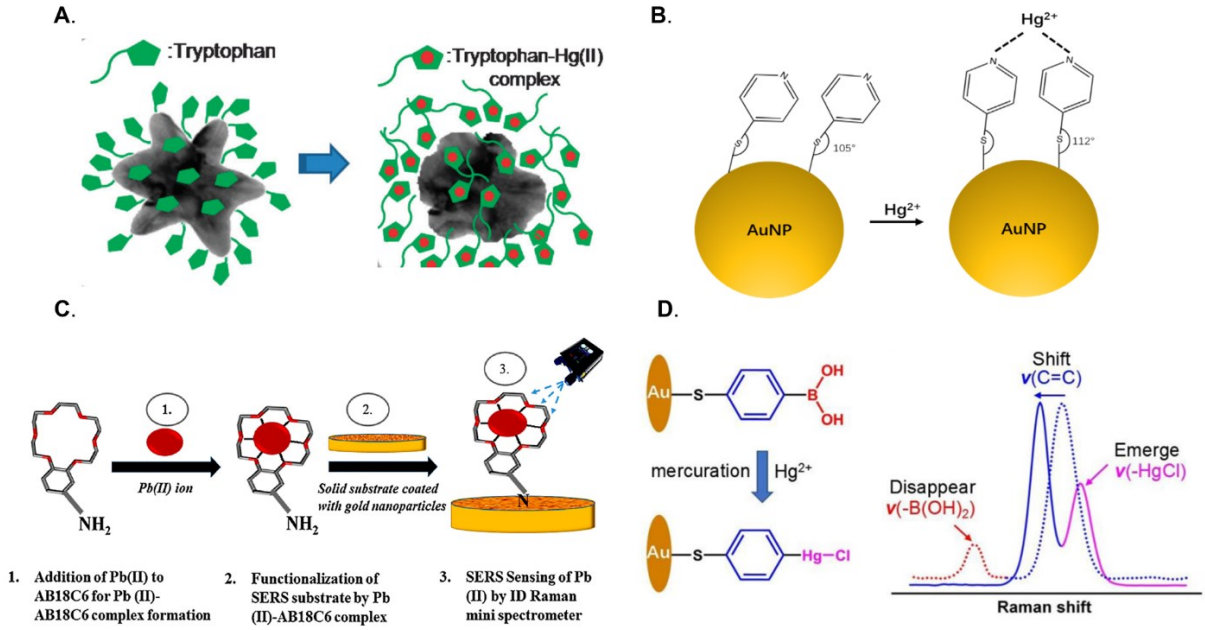

Figure 2.4 Reporter molecular recognition based on reporter molecule (A) displacement, adopted from Senapati et al., (2011); (B) re-orientation, adopted from Guo et al., (2020) and structure change with (C) addition, adopted from Sarfo et al., (2018); (D) substitution reaction between the reporter molecule and the metal ions, adopted from Zhao et al., (2020).

The reporter molecule also can be re-orientated on the substrate surface upon the interaction with analyte metal ions, which is based on the surface selection rules of SERS. The surface selection rules of SERS demand that for the adsorbed molecule on the SERS substrate surface, only those vibration modes where the direction of polarizability change is consistent with the enhanced electromagnetic field can exhibit the high SERS enhancement (Pérez-Jiménez et al., 2020). Therefore, when the metal ions interact with reporter molecule and cause the orientation change of reporter molecule, the SERS signal intensity of the reporter molecule can also be changed. For example, 4-Mercaptopyridine (4-Mpy) is a small organic ligand which contains a thiol group and the pyridine moiety, which can coordinate with metal ions to result in the redistribution of electrons within the aromatic ring structure (Mizutani & Ushioda, 1989). The pyridinic N atoms especially could coordinate with Hg^{2+} where the N acts as an σ-electron donor (Ibusuki & Saito, 1976). After adsorbing 4-Mpy on indium tin oxide (ITO) glass assembled AuNPs via an Au-S bond, the N atom in pyridine is available for Hg^{2+} selective coordination. One Hg^{2+} ions can strongly interact with two adjacent pyridine ring N atoms to form the metal complex. Because of the metal complex formation, the orientation of 4-Mpy is changed, with the 4-Mpy molecules now “standing” more perpendicularly on AuNPs surface. Density functional theory (DFT) calculations suggested that the intersection angle of C-S-Au increased by 7°, from 105° to 112° (as shown in Figure 2.4B), which puts the reoriented 4-Mpy molecule in greater agreement with surface selection rules. Subsequently, most of the vibrational modes of 4-MPY are intensively increased and thus the overall enhanced SERS spectra of 4-Mpy can be observed. In particular, the most intensive enhancement was observed for the pyridine breathing vibration

mode at 1093 cm^{-1} peak position, which was used for quantitative analysis (Guo et al., 2020). The high affinity between the pyridinic N atoms of the 4-Mpy and Hg^{2+} prevents interference from other cations and anions, which enable good selectivity of the SERS sensor. Instead of using the commercially available molecule 4-Mpy, synthesized histidine (H) conjugated perylene diimide (PDI) bolaamphiphile (HPH) could also work in a similar way for selectively Hg^{2+} sensing (Makam et al., 2018). The functional group, -NH, enables HPH to be strongly immobilized onto Au-deposited monodispersed nanospheres monolayers (Au-MNM) of polystyrene substrate surface and the -NH group at the other end of HPH remains free and flexible for Hg^{2+} interaction. The chelation between HPH and Hg^{2+} involves two neighboring HPH molecules and one Hg^{2+} ion, which form a host-guest complex on the surface of Au-MNM. An overall enhancement of the SERS signal of HPH upon the addition of Hg^{2+} was observed. Plus, by using HPH, this SERS metal sensor also can be used as a fluorescence sensor (Makam et al., 2018). It is worth noting that a relative high surface coverage of the reporter molecules was required. The high density of the monolayer on the substrate surface likely prevents the target metal ions from interacting with the binding site between the reporter molecule and substrate.

The interaction between metal ions and the active binding site of the reporter molecules causes the structural change of the reporter molecules as well. This includes metal ions forming a complex or substitution reactions between the metal ions and certain functional groups of the reporter molecule. For these, the structure change of the reporter molecules is spectrally visible, which is usually shown by the partial spectra region alteration, *e.g.,* new peak, peak shift, peak disappear (Awual et al., 2014; Zhao et al., 2020).

Crown ethers, including their derivates, can form metal complexes through ion-dipole interactions with metal cations (Awual et al., 2014). Notable, benzo-18-crown-6 can selectively interact with Pb^{2+} to form a stable complex. By engineering the amino group on benzo-18-crown-6, the aminobenzo-18-crown-6 (AB18C6) could be immobilized on a gold nanostructured substrate via an Au-N bond and could use for the selective sensing of Pb^{2+} as shown in Figure 2.4C. As a result, compared to AB18C6, the SERS spectra of the Pb-AB18C6 complex showed several new peaks and peak shifts because of the vibrational modes change, where the new peak of 820 cm^{-1} is attributed to the crown ether-Pb complex and is most sensitive to the Pb^{2+} concentration (Sarfo et al., 2018). Similarly, a crown ether derivative was also synthesized by the coupling of aminodibenzo-18-crown-6 (ADB18C6) and mercaptopropionic acid, which was used for Hg^{2+} detection (Sarfo et al., 2017).

The reporter molecule structure can also be changed by substituting its functional groups upon the interaction with target metal ions. For example, as shown in Figure 2.4D, 4-mercaptophenylboronic acid (4-MBA) could be used as a multifunctional SERS reporter, since it contains a thiol binding component, an aromatic Raman-active nucleus, and a substitution trapping moiety (Zhao et al., 2020). Hg^{2+} can interact with the trapping moiety of 4-MBA resulting in the $-B(OH)_2$ moiety being substituted by a -HgCl group to form 4-mercaptophenyl mercury chloride (4-MMC). Because of this geometric reconstruction, the boron-related vibrations disappear whereas the mercury monochloride group could be observed. In addition, by directly binding of Hg, the polarizability of aromatic nucleus was increased, which results a significant peak shift of C=C from 1636 cm^{-1} to 1588 cm^{-1}.

A variety of metal ions can be detected using a variety of reporter molecular recognition systems (Table 1). The SERS substrates commonly include variation of gold and gold or silver nanoparticles with a diversity of reporter molecules.

Table 1. Metal ion detection based on the reporter molecular recognition.

Metal	SERS substrate	Reporter molecule	Ref
Cu^{2+}	AuNP	dipicolylamine	(Dugandžić et al., 2019)
Zn^{2+}	Au nanoarray	2-carboxyl-2'-hydroxyl-5'-sulfoformazylbenze	(Teng et al., 2020)
Cd^{2+}	AgNP	phenylmethanethiol-terpyridine	(Cheng et al., 2015)
Hg^{2+}	AgNP chip	Dimethyldithiocarbamic acid sodium salt	(Chen et al., 2016)
Hg^{2+}	Au	Aminodibenzo-18-crown-6	(Sarfo et al., 2017)
Hg^{2+}	Au@Ag@SiO2	-NH2-R6G-CHO	(Ma et al., 2015)
Hg^{2+}	AuNS@Ag	rhodamine derivatives	(Li et al., 2018)
Hg^{2+}	AuNP	p-methylcarbohydrazonethioamide	(Franciscato et al., 2018)
Hg^{2+}	AuNR-PCL	2,5-dimercapto-1,3,4-thiadiazole dimer	(Tang et al., 2015)
Cu^{2+}		Trimercaptotriazine	
Hg^{2+} Cd^{2+}	AuNP	Trimercaptotriazine	(Zamarion et al., 2008)
Mn^{2+}			
Ni^{2+} Cu^{2+}	AgNP	Salen	(Docherty et al., 2016)
Co^{2+},			
Fe^{2+}	AgNP	2,2'-bipyridyl	(Docherty et al., 2015)

Ni^{2+}			
Zn^{2+}			
Cu^{2+}			
Cr^{3+}			
Cd^{2+}			
Hg^{2+}	AuNP	2-Mercaptoisonicotinic acid	(Tan et al., 2012)
Pb^{2+}			
Al^{3+}			
Sb^{2+}			
As^{2+}	AgNP	poly(propylene amine)-naphthalimide	(Temiz et al., 2013)
Cd^{2+}			
Pb^{2+}			
K^{+}			
Pb^{2+}	AuNR	4-Mercaptobenzoic acid	(Ho et al., 2019)
Fe^{3+}			
Fe^{3+}			
Cr^{3+}			
Mn^{2+}	Au	Cyanide	(Kim et al., 2013)
Fe^{2+}			
Co^{2+}			
Ni^{2+}			

2.3.2 Inter-substrate Distance Change

The interaction between an analyte metal ion and the capturing agent can induce a change in the inter-substrate distance. Generally, as shown in Figure 2.5A, without any target metal ions, coinage metal nanoparticles, with the adsorbed reporter molecules and capturing agent, are well dispersed in solution. When the analyte metal ions are introduced however, the capturing agent adsorbed on the nanoparticle can recognize the presence of metal ions and immediately interact with them. Because of the binding of the capturing agent with metal ions, adjacent nanoparticles can overcome their inherent repulsive forces and approach close to each other. This induces the generation of numerous nanogaps within each aggregate, thus placing the reporter molecules in the nanogaps. Since the electromagnetic field can be dramatically enhanced within the nanogaps, which are also known as hot spots, the SERS signal intensity of the reporter molecule is consequentially enhanced, leading to a "turn-on" metal sensor. In contrast, a "turn-off" sensor can be constructed by reversing the mechanism (Figure 2.5B), wherein the addition of metal ions can disaggregate pre-formed nanoaggregates and thus attenuate reporters signal intensity. The degree of aggregation or disaggregation of the SERS substrate in both cases is dependent on the metal ion concentration, which also enables quantification using this type of sensor. In addition, the inter-substrate distance change is also a mechanism applied in nanoparticle based colorimetric sensors. Therefore, some metal ions sensors based on inter-substrate distance change can be constructed as dual-mode SERS and colorimetric sensors, which can achieve low-concentration detection as well as expand the detection range at the same time as the colorimetric sensor has different linear detection range when compared to the SERS sensor.

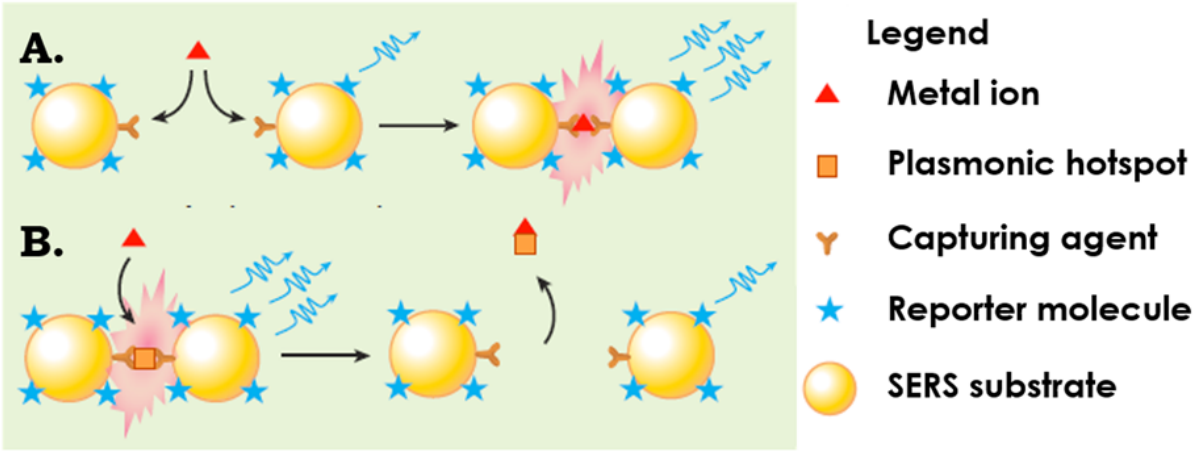

Figure 2.5 (A) Metal ion induces NPs aggregation and hot spot generation; (B) Metal ions induce disaggregation of NPs aggregate and disband hot spot. Adopted from Gu et al., (2018).

2.3.2.1 Reporter Molecules Serving as Capturing Agent.

Some reporter molecules not only have a Raman active moiety, but also have functional groups that are capable of chelating metal ions, allowing those reporter molecules to act as a multi-functional molecule in metal sensors. For example, some capping agents used in nanoparticle synthesis can be directly used as reporter molecules for metal ions detection. Citrate molecules are widely used for AgNPs or AuNPs synthesis, acting as both the reducing agent and capping agent. It has been found that citrate reduced AuNPs can be directly used for Pb^{2+} sensing without further surface modification, where the carboxylate and hydroxyl groups of citrates have a high affinity towards Pb^{2+} (Frost et al., 2015). In addition to citrate, poly(vinylpyrrolidone) (PVP) is a neutral polymer that can help nucleation and growth during the metal NP synthesis (Kedia & Senthil, 2012). PVP stabilized AgNPs can be used for Cu^{2+} detection, where the N and O atoms of PVP coordinate with Cu^{2+} and cause pyrrolidinone ring torsion in PVP (Xu et al., 2019). Both citrate and PVP play three

key roles in SERS metal sensors, which are capping of the substrate, the capturing of target metal ions, and serving as reporter molecules to generate SERS signals. Such versatile properties of the reporter molecule enable a simple SERS metal sensor because the as-synthesized substrates can be directly used for metal ions detection without any further functionalization. However, the as-synthesized nanoparticles may suffer nonspecific aggregation in aqueous solution and give false positive SERS signals of the reporter molecule, which affects the selectivity and accuracy of the sensor.

Surface modification of the substrate with multi-functional reporter molecules promotes the sensor to be more selective towards the target metal ions. For instance, 2,5-Dimercapto-1,3,4-thiadiazole (DMcT) can replace citrate and strongly adsorb on Au@Ag NPs surface through two Ag-S covalent bonds and form a monolayer on the substrate surface as shown in Figure 2.6A. In the presence of Hg^{2+}, two N atoms with lone pair electrons DMcT show strong interactions with Hg^{2+} and form a Hg-N complex. This complexation places the DMcT in the hot spots of the assembled Au@Ag NP aggregates, leading to a "turn-on" SERS signal for DMcT. In addition, DMcT functionalized substrates show a strong resistance against other interfering metal ions, including Pb^{2+}, Cd^{2+}, Fe^{2+}, Al^{3+}, Fe^{3+}, Cu^{2+}, Na^{+}, Cr^{3+}, Zn^{2+}, Mg^{2+}, Ca^{2+} and Co^{2+} (Zeng et al., 2017). By taking advantage of the high stability constant of the Hg-N complex, 4,4'-Dipyridyl (Dpy) linked Au@Ag NP aggregates have also been utilized to construct a "turn-off" SERS sensor (Figure 2.6B). In addition to the hot spot removal, the reporter molecule, Dpy, was released from the Au@Ag NPs surface upon the interaction with Hg^{2+}, which improves the sensitivity of this sensor up to 10^{-14} M (10 fM) (Du et al., 2013).

Two types of multi-functional reporter molecules can be simultaneously used to specifically coordinate with certain metal ions. For example, 4-Mercaptobenzoic acid (4-MBA) and 4-Mercaptopyridine (4-Mpy) both contain a thiol binding group, Raman active moiety, and capturing functional group. The pyridyl nitrogen of 4-Mpy and carboxy group of 4-MBA can specifically coordinate with Cu^{2+} at 2:1 molar ratio. Therefore, in the presence of Cu^{2+}, the 4-MBA functionalized AgNPs (AgNPs-MBA) and the 4-Mpy functionalized AuNPs (AuNPs-Mpy) can form core-satellite structures, generating hot spots between the AuNPs and AgNPs (Figure 2.6C) (Guo et al., 2020). In addition to the general enhanced signals, the peaks associating with pyridyl nitrogen and COO^- symmetric stretching have become significantly more intense upon the binding of Cu^{2+} (Guo et al., 2020). Metal ion detection using two characteristic peaks from two reporter molecules can improve the selectivity of the sensor and reduce the probability of giving false-positive signals.

The use of multi-functional reporter molecules in SERS metal sensors allows for simple construction, easy operation and rapid detection. However, the type of multi-functional reporter molecules that can be used, and the metal ions can be detected by multi-functional reporter molecules, are highly limited. In addition, the Raman active moiety and the capturing group of a multi-functional molecule typically do not have the same high-level performance at the same time, which influences sensitivity or selectivity of the sensor. Therefore, different reporter molecules with different capturing agents are more commonly used in constructing SERS metal sensors in order to have a better control and performance in both sensitivity and selectivity.

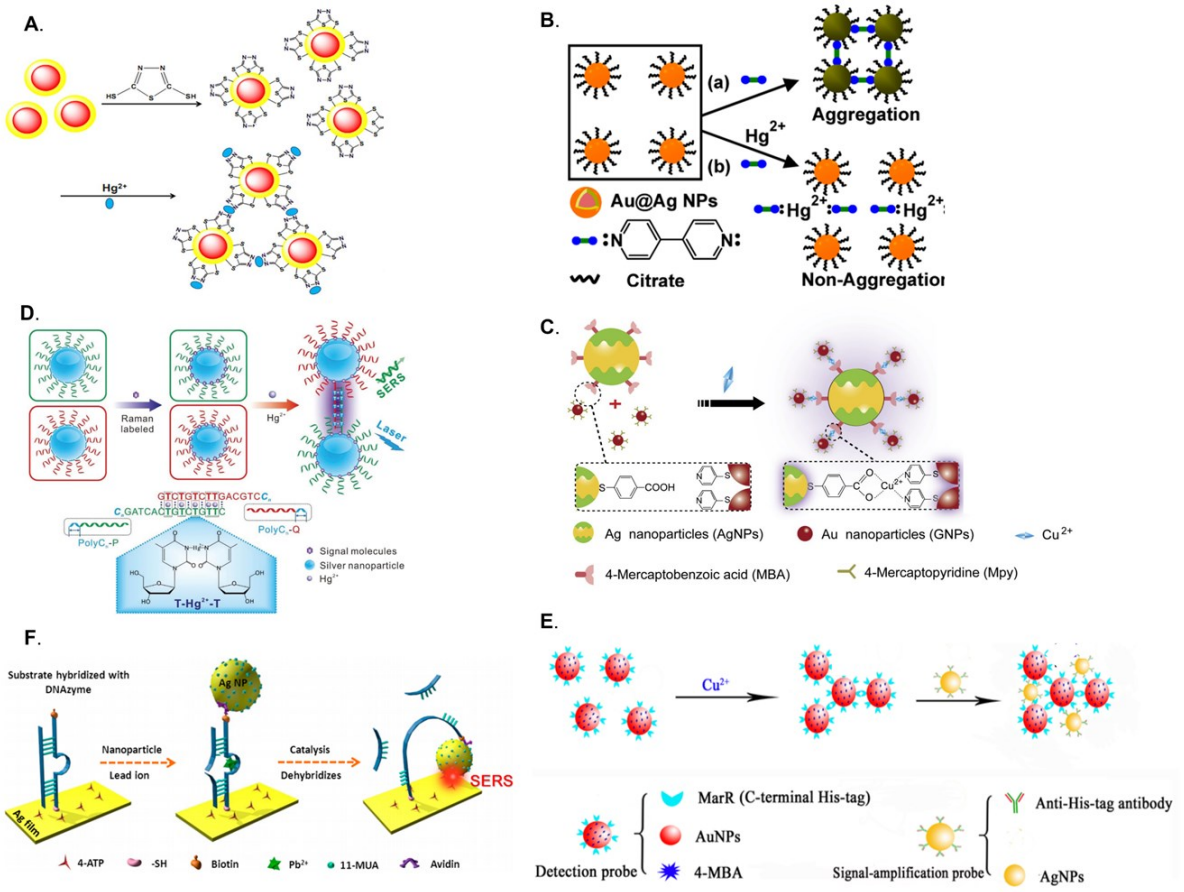

Figure 2.6 Reporter molecules serving as capturing agent for (A) "turn-on" Hg^{2+} SERS sensor, adopted from Zeng et al., (2017), and (B) "turn-off" Hg^{2+} SERS sensor, adopted from Du et al., (2013); (C) using two reporter molecules for Cu^{2+} sensing, adopted from Guo et al., (2020); (D) DNA as capturing agent for Hg^{2+} sensing, adopted from Qi et al., (2017); (E) Pb^{2+} specific DNAzyme linked two substrates with different morphology, adopted from Fu et al., (2014); (F) Cu^{2+} specific protein as capturing agent and dual hot spot formation, adopted from Wang et al., (2017) for SERS metal sensors.

2.3.2.2 Other Molecules Serving as Capturing Agent.

The selection for capturing agents indicate that it should have a high selectivity towards the target metal ions. In addition, the ideal capturing agent should have no Raman activity, which can eliminate interference with the reporter molecule. On the other hand, reporter molecules

should have a simple molecular structure, a high Raman activity moiety, strong binding with the substrate, and be sensitive to the surrounding environment such that the change in the SERS signal can be easily monitored (Sun et al., 2017).. In addition, the capturing agent adsorption should not cause significant dissociation of reporter molecules from the substrate surface.

The capturing agents used in SERS metal sensors includes a variety of small molecules and polymers. For example, glutathione (GSH) can adsorb on AgNPs surface through Ag-S bonds and can specifically bind with As^{3+} through an As-O linkage. This can induce NP aggregation and enhance the SERS signal of 4-Mpy (Li et al., 2011). Similarly, gluconate ions show a specific affinity towards Pb^{2+} when the gluconate ions are adsorbed onto Au@AgNPs surfaces, wherein 2-Naphthalenethiol (2-NT) acts as the reporter molecule (Zhang et al., 2019). In addition to small molecules, engineered polymers also can be selectively used for metal ions detection. For example, a specific Cd^{2+}-chelating polymer layer formed on AuNPs surface via surface-initiated atom transfer radical polymerization can stabilize the AuNPs and prevent the nonspecific aggregation when in the absence of Cd^{2+}. When the interaction with Cd^{2+} occurs, the polymer can recognize Cd^{2+} via specific metal-ligand interactions and lead to AuNPs aggregation (Yin et al., 2011).

Single DNA strands as a special type of polymer also have been widely used as capturing agents, based on the strongly specific recognition between certain bases and target metal ions such as thymidine-Hg^{2+}-thymidine (T-Hg^{2+}-T) coordination and cytosine-Ag^{+}-cytosine (C-Ag^{+}-C) coordination. Two partly complementary T-rich or C-rich single DNA strand functionalized SERS substrates can interact with Hg^{2+} or Ag^{+} to form a mismatched

DNA duplex, which bridges two substrates and decrease the distance between them. T-rich thiolated DNA strands can capture Hg^{2+} and form Au nanostar (AuNSs) dimers (Ma et al., 2013). Similarly, upon the addition of Hg^{2+}, T-rich thiolated DNA can bridge AuNPs and Au nanorods (AuNRs) to form nanochain and nanorod side-by-side assemblies, respectively, with the length of both nanostructures being dependent on the Hg^{2+} concentration (Wu et al., 2015; Xu et al., 2015). Comparing to thiolated DNA, AgNPs functionalized by Poly-cytosine (polyC) DNA show good stability under high ionic strength (Qi et al., 2017). In addition, by taking advantage of intrinsic silver-cytosine (Ag-C) coordination (Lu et al., 2017), the DNA density on the AgNP surface can be tuned by adjusting the length of polyC, which can affect the formation of the T-Hg^{2+}-T bridges and the degree of inter-AgNPs distance changeas, shown in Figure 2.6D (Qi et al., 2017).

Additionally, DNA strands acting as the capturing agent can be utilized to change the distance between colloidal metal nanoparticles and a solid metal substrate upon the interaction with analyte metal ions, including Pb^{2+} specific DNAzyme and T-Hg^{2+}-T or C-Ag^{+}-C mismatched DNA duplexes (Fu et al., 2014; Zheng et al., 2015). For example, Fu et al., constructed a rigid double-stranded 17DS DNAzyme for Pb^{2+} specific SERS sensing, where the DNAzyme was connected to the AgNPs and a solid Ag film at its 3' and 5' ends via thiol groups and biotin, respectively (Figure 2.6E). The AgNPs were functionalized with a spacer molecule, 11-mercaptoundecanoic acid (11-MUA; 1.25 nm in length), and a reporter molecule, 4-aminothiophenol (4-ATP; 0.67 nm) was located randomly on the Ag film surface. Upon the interaction with Pb^{2+}, the DNAzyme became flexible and the AgNPs fell to the surface of the Ag film forming a nanogap of about 2.19 nm, such that the 4-ATP could

generate a “turn-on” SERS signal (Fu et al., 2014). 17DS DNAzymes can also be utilized in “turn-off” SERS sensors for Pb^{2+} detection. The thiolated DNAzyme immobilized on Au-coated substrate surface and the cleavage substrate is hybridized with DNAzyme to form double-strand DNAzyme. By extending the 5’ end of the cleavage substrate, the AuNPs co-functionalized with the reporter molecule 4-MBA and the short single strand DNA (complementary to the extension of 5’ end) can be attached and form a narrow gap between the AuNPs the Au-coated surface (Wang & Irudayaraj, 2011). The specific catalytic reaction between the DNAzyme and Pb^{2+} leads to the cleavage of the AuNPs from the Au-coated surface, eliminating the narrow gap and resulting in a decreased SERS signal for 4-MBA.

A dual hot spots strategy can also be applied to improve the sensitivity of SERS metal sensors. At low concentrations, the amount of hot spot generated by analyte metal ions interacting with a capturing agent may not be able to support significant enhancement of the SERS signal. The formation of extra hot spot regions that amplify the SERS signals of reporter molecules can improve the sensitivity of SERS metal sensors. As an example, multiple antibiotic resistance regulator (MarR), also known as C-terminal His-tag, functionalized AuNPs can be used for Cu^{2+} specific recognition, where Cu^{2+} induces the oxidation of the cysteine residue to generate disulfide bonds between two MarR dimers (Wang et al., 2017). The dual hot spots can be formed by using Anti-His-tag antibody coated AgNPs to combine with AuNPs through antigen-antibody reactions (see Figure 2.6F). The hot spots between AuNPs induced Cu^{2+} plus the hot spots between AuNP-AgNP heterodimers generate significantly enhance SERS signals of the reporter molecule 4-MBA, which improves the sensitivity of the sensor by 50-fold (Wang et al., 2017).

More examples of inter-substrate distance change-based SERS metal sensors are summarized and listed in Table 2. Gold and silver nanoparticles are commonly used as substrates with a diversity of reporter and capture agents.

Table 2. SERS metal sensors based on the inter-substrate distance change.

Metal	Substrate	Reporter	Capturing agent	Signal	LOD	Range	Ref
Cu^{2+}	AuNSs	L-cysteine	--	on	10 uM	N/A	(Ndokoye et al., 2014)
Hg^{2+}	AuNPs	Bismuthiol II	--	off	30 nM	30 nM - 150 nM	(Duan et al., 2012)
Zn^{2+}	AuNPs	MDPA	--	on	280 fM	6 uM – 200 uM	(Li et al., 2018)
Cu^{2+}	AuNRs	Binaphthalene	--	on	380 fM	1 uM - 100 uM	(Zheng et al., 2020)
Hg^{2+}	AuNPs	4-MBA	--	on	25 pM	20 pM - 2.5 uM	(Zheng et al., 2017)
Pb^{2+}	Au@Ag NPs	4-ATP	L-cysteine	on	1 pM	5 pM – 10 nM	(Xu et al., 2018)
As^{3+}	Au@Ag NPs	4-MBA	DNA aptamer	on	1.3 nM	67 nM - 133 nM	(Song et al., 2016)
As^{3+}	AuNPs	R6G	Glutathione	on	1.5 nM	1.5 nM – 66.7 nM	(Li et al., 2020)
As^{3+}	Au@Ag NPs	4-Mpy	DNA aptamer	on	786 pM	1.3 nM – 1.3 M	(Yang et al., 2015)
Cu^{2+}	AgNPs	R6G	L-cys/IP6	off	10 pM	100 pM - 1 uM	(Liu et al., 2019)
Cd^{2+}	AuNPs	Alizarin dye	Aggregation	on	50 pM	N/A	(Dasary et al., 2016)
Cu^{2+}	AgNPs	3,5-Dimethoxy-4-(6'-zaobenzotriazolyl) pnenol	L-cysteine	on	10 pM	N/A	(Li et al., 2013)
Hg^{2+}					1 pM	N/A	
Ag^{+}	AuNSs /	MGITC	DNA aptamer	on	1.7 pM	2 pM – 10 nM	(Zheng et al., 2015)

Hg^{2+}	Au nanohole array				2.3 pM	5 pM – 100 nM	
Cr^{3+}	AuNPs	2-ATP	Citrate	on	50 nM	N/A	(Ye et al., 2012)

2.3.3 Reporter Molecule Location Change

Under this mechanism, instead of adsorbing onto the substrate surface, the reporter molecule is connected to the substrate by a capturing agent (DNA). When interacting with analyte metal ions, the capturing agent undergoes a conformation change. This changes the location of the reporter molecules such that the reporter molecule either moves closer to or away from the substrate surface, resulting in a respective change in the SERS signal of the reporter. The electromagnetic field generated by the localized surface plasmon resonance (LSPR) of the SERS substrate surface is distance dependent, where the electromagnetic enhancement and SERS signals decays exponentially with distance from the SERS substrate surface (Pilot et al., 2019). Therefore, when the reporter molecules are located near the substrate surface, they can experience a stronger electromagnetic enhancement and give a more intensive SERS signal than when the reporter molecules are located far from the substrate surface. DNA possesses several advantages as a capturing agent for metal ions. For example, DNA has multiple modes for potential metal binding and significant changes in DNA conformation can occur upon the binding of metal ions (Zhou et al., 2017). Therefore, by taking advantage of DNA as a metal ion capturing agent and combining the distance-dependent property of SERS signals, a SERS metal sensor can be constructed. The reporter molecule can be functionalized with DNA so that it can regulate its location from the SERS substrate surface

based on the conformational state of the DNA after interacting with metal ions. Depending on the way the DNA conformation changes, either “turn-on” or “turn-off” SERS metal sensors can be constructed.

There are generally two types of functional DNA developed for metal ions detection; aptamers, designed directly for selective metal binding, and DNAzymes, based around metal-assisted DNA catalysis (Zhou et al., 2017). The aptamers used as the capturing agent in SERS metal sensors are based on the coordination between Hg^{2+} and thymine (T), or Ag^{+} and cytosine (C) (Miyake et al., 2006; Ono et al., 2008). Because of these intrinsic interactions, T-rich and C-rich DNA aptamers can specifically interact with Hg^{2+} and Ag^{+} to form T-Hg^{2+}-T and C-Ag^{+}-C mismatched base pairs forming either folded hairpin structures or rigid sandwich structures (Ding et al., 2013; Han et al., 2010; Wu et al., 2018). DNAzymes are functional single stranded DNA sequences with enzyme-like catalytic activity that is highly dependent on specific cofactors including proteins and metal ions (Gong et al., 2015). After activation by its cofactors, DNAzymes can cleave its substrate strand at the adenine ribonucleotide (rA) site (Morrison et al., 2018). For example, the “8-17”-DNAzyme is well-established for its high affinity towards Pb^{2+}, where in the presence of Pb^{2+}, the “8-17” DNAzyme can be activated to cleave its substrate strand into two fragments (Yang et al., 2017). Depending on where the reporter molecule labeling site on is the DNAzyme, both “turn-on” and “turn-off” SERS sensors can be constructed.

2.3.3.1 DNA Aptamer Conformation Change Induced Reporter Location Change.

When a single DNA aptamer interacts with analyte metal ions it can fold to form a hairpin structure wherein the metal ions are captured and bonded within. For example, a T-rich

single DNA aptamer with thiol group and cyanine (Cy5) have been functionalized at 3' and 5' end, respectively (Sun et al., 2015) (as shown in Figure 2.7A). The thiolated 3' end is immobilized on AuNPs decorated silicon nanowire array (AuNPs@SiNWAr) which leaves the reporter molecule Cy5 far from the substrate surface. By interacting with Hg^{2+} and forming the hairpin structure, the location of Cy5 is moved close to the AuNPs@SiNWAr surface, resulting in a "turn-on" SERS signal (Sun et al., 2015). In contrast, a T-Hg^{2+}-T based hairpin structure can be used for sig "turn-off" sensors. For example, a single walled carbon nanotube (SWCNT) has been utilized as a reporter and bound to a T-rich single DNA strange through π-π interactions. However, as shown in Figure 2.7B, in the presence of Hg^{2+}, due to the strong coordination between Hg^{2+} and T and the resulting hairpin structure, the SWCNT was released from the substrate surface, resulting in a decreased SERS signal (Yang et al., 2017).

In another approach, two single stranded DNA aptamers can form a sandwich structure, which is based on metal triggered mismatched base pairs (instead of the conventional Watson–Crick base pairing). For example, a sensor was developed where thiolated DNA1 was adsorbed on the SERS substrate surface while the reporter, tetramethylrhodimine (TAMRA) tagged DNA2, was suspended in the solution (Figure 2.7C). Because of the coordination between T and Hg^{2+}, in the presence of Hg^{2+}, DNA2 is captured and forms T-Hg^{2+}-T mismatched pairs with DNA1, resulting in a sandwich structure of DNA1-Hg-DNA2. As a result, the TAMRA molecule is brought to substrate surface and creates a "turn-on" SERS signal (Zhang et al., 2017). Similarly, in another approach (Figure 2.7D), single stranded DNA containing 15 thymines adsorbed on silver nanorods array (via

Ag-S bonds) was combined with a reporter, Cy5 at the 3'-end. The flexibility of this single stranded DNA allowed Cy5 to stay near to the substrate surface. However, the presence of Hg^{2+}, the two adjacent DNA strands form a rigid sandwich structure. This causes the DNA strands to "stand" on the substrate instead of "laying" on the surface. As a result, the Cy5 move away from the silver nanorod surface, leading to a decreased SERS signal (Song et al., 2017).

In addition to single DNA aptamer formed hairpin structures, pre-formed hybridized double DNA strands can also be converted to hairpin structures with labelled reporter molecules either adsorbed on the SERS substrate surface or released in the solution. For example, as shown in Figure 2.6E, Au@Ag core-shell NPs were firstly functionalized with thiolated 5′-Rox C-containing labeled aptamer (Rox aptamer). Following hybridization with its complementary DNA (cDNA), these can form a rigid double strand DNA on the substrate surface, where the reporter Rox is far from the surface. In the presence of Ag^{+}, the rigid double strand DNA is converted to a Rox aptamer formed hairpin structure because of the C-Ag^{+}-C mediated base pairs and the reporter Rox is brought to Au@Ag NPs surface while the cDNA is released in solutions, resulting in a "turn-on" SERS signals (Wu et al., 2018). In contrast, the formed hairpin structure with reporter labelling can be released in solutions upon the interaction with metal ions, which can be used as a "turn-off" SERS metal sensor. As seen in Figure 2.7F, a DNA aptamer can be functionalized with a thiol group at its 3'-end and immobilized on Au core surface via Au-S covalent bond (Chung et al., 2013). After being decorated with an Ag shell on the Au core surface, the thiolated DNA aptamer can partially hybridized with its complementary DNA aptamer that contains T-rich bases and a

Cy3 label at the 3'-end, forming a rigid double stranded DNA segment. By optimizing the thickness of Ag shell, the Cy3 can be located very close to the substrate surface and have a strong SERS signal. However, with the interaction Hg^{2+}, the T-rich and Cy3 labeled DNA aptamer is dehybridized and forms a hairpin structure. Thus, the Cy3 was released from the substrate surface and resulted in a decreased SERS signal (Chung et al., 2013).

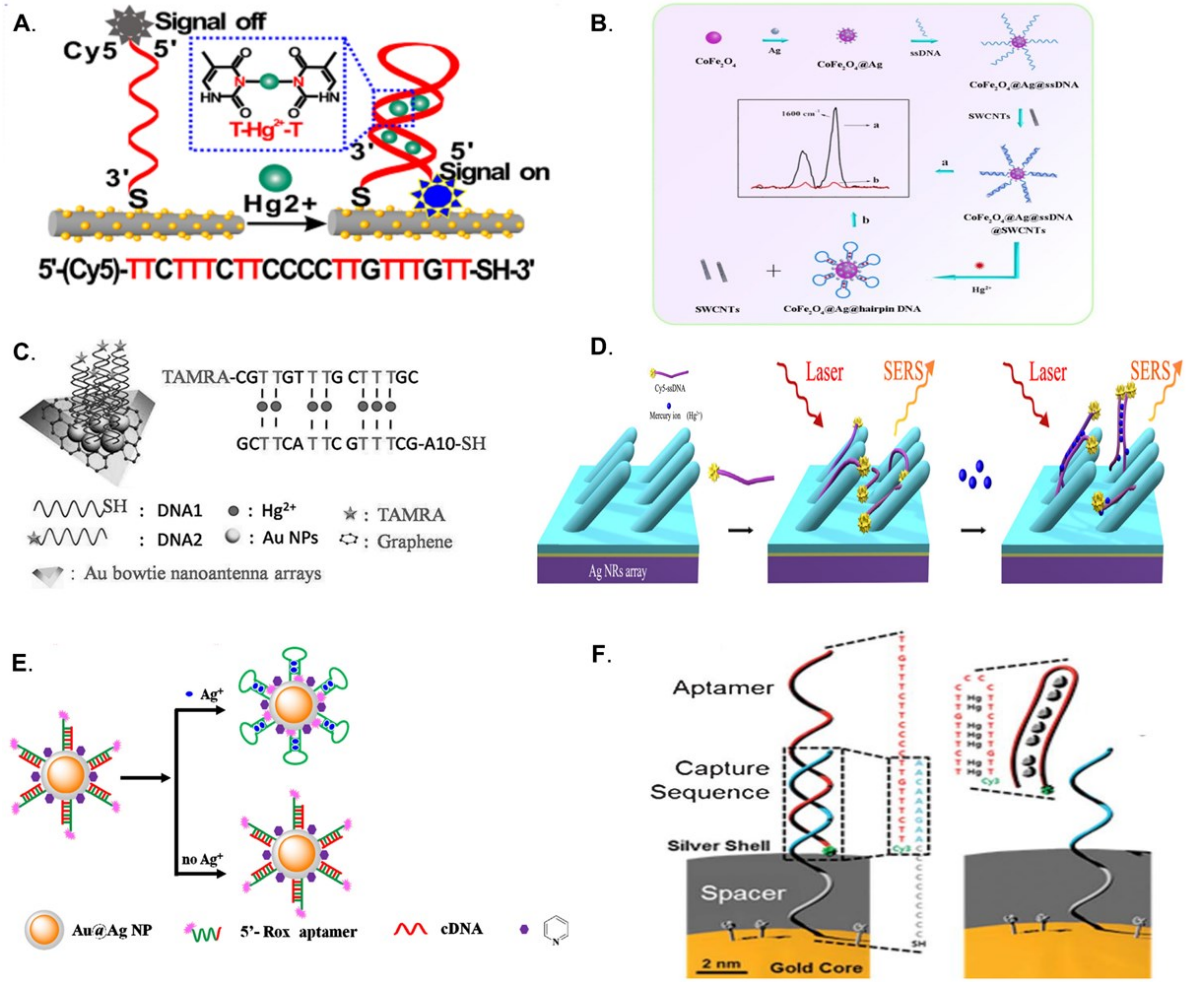

Figure 2.7 Hairpin structure DNA aptamer used for (A) "turn-on" Hg^{2+} sensor, adopted from Sun et al., (2015); and (B) "turn-off" Hg^{2+} sensor, adopted from Yang et al., (2017). Sandwich structure DNA aptamer used for (C) "turn-on" Hg^{2+} sensor, adopted from Zhang et al., (2017); and (D) "turn-off" Ag^{+} sensor, adopted from Song et al., (2017), SERS metal

sensors. Double strand DNA aptamer switched to hairpin structure for both (E) "turn-on" Ag^{+} sensor, adopted from Wu et al., (2018); and (F) "turn-off" Hg^{2+} sensor, adopted from Chung et al., (2013).

2.3.3.2 DNAzymes Cleavage Causing Reporter Location Change

Unlike with the direct binding of DNA aptamers, DNAzyme based metal ion detection relies on the role of the metal ions acting as a cofactor for activating catalytic processes. For example, the secondary structure of "8-17" DNAzyme is shown in Figure 2.8. The "8-17" DNAzyme consists of an enzyme strand (17E) and its substrate strand (17DS), where the cleavage site of Pb^{2+} is located on 17DS (Liu & Lu, 2004). When the DNAzyme is activated by Pb^{2+}, it will be dehybridized and cleave its substrate strand into two fragments, resulting in the enzyme strand becoming flexible (Liu & Lu, 2004). Based on this property, DNAzymes have been utilized as capturing agents to construct SERS metal sensors.

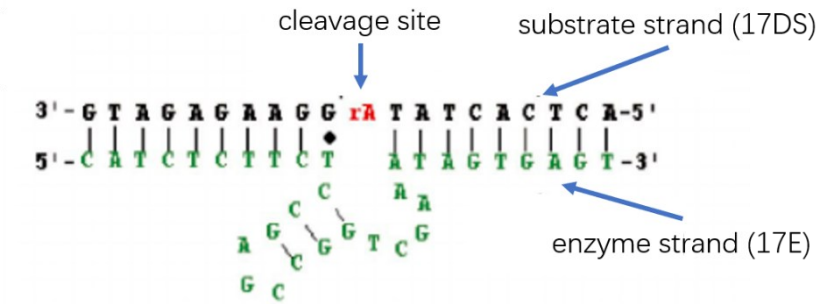

Figure 2.8 Secondary structure of "8-17" DNAzyme. Adapted from Liu and Lu, (2004).

The specific binding sites of the reporter molecule bound to the DNAzyme determines if the sensor has either a "turn-on" or "turn-off" signal. For example, in a "8-17" DNAzyme, there are two binding sites for both the substrate strand and enzyme strands. Except for one binding site for adsorbing on SERS substrate surface, there are a total three

binding sites for reporter molecules. If the enzyme strand was functionalized with a binding group, usually a thiol group, and labeled with reporter molecules, a "turn-on" SERS sensor can be constructed, where after the interaction with Pb^{2+}, the enzyme strand becomes flexible and can bring the reporter close to the substrate surface. As shown in Figure 2.9A, an enzyme strand was functionalized with thiol group and Cy5 at 5' and 3' end, respectively. In the absence of Pb^{2+}, because of the rigid double DNA strand, the Cy5 is located far from the substrate surface. However, with the interaction of target metal ions, the 17DS substrate strand is cleaved and 17E enzyme strand becomes flexible allowing the reporter Cy5 to approach to the substrate surface, leading to a "turn-on" SERS signals (Shi et al., 2016). On the other hand, if the reporter is tagged on the substrate strand, either on the 3' or 5' end, a "turn-off" SERS sensor can be constructed, since after the cleavage, the substrate strand will be released from the substrate surface resulting a decreased SERS signals of the reporter molecule. For example (as shown in Figure 2.9B), when the 17DS substrate strand was functionalized with a thiol group at 5'-end that can adsorb on the AuNRs surface via Au-S bond, the reporter, Cy5, can be labeled at the 3'-end. Before the activation by Pb^{2+}, the SERS signal Cy5 can be obtained but in the presence of Pb^{2+}, the 17DS substrate strand is cleaved and the fragment with Cy5 labeling is released from the AuNRs surface, resulting in a decreased SERS signal (Xu et al., 2019).

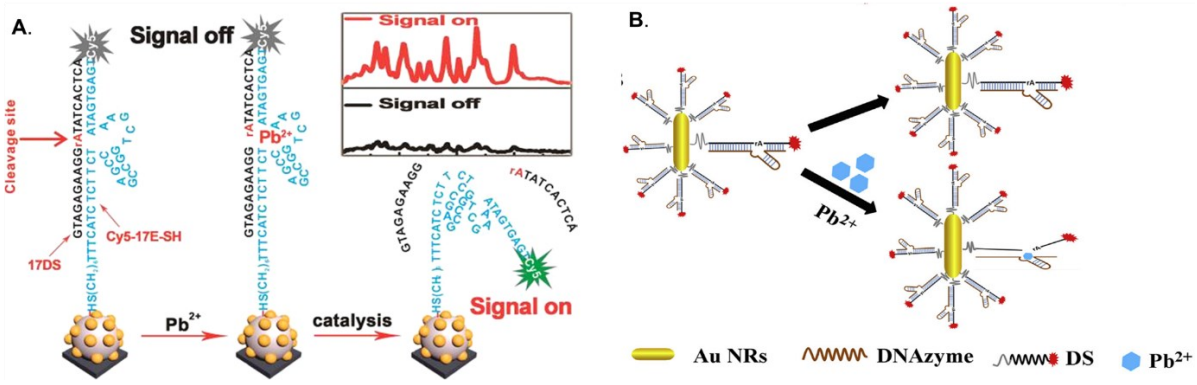

Figure 2.9 "8-17" DNAzyme based Pb^{2+} SERS sensor with (A) "turn-on", adopted from Shi et al., (2016); and (B) "turn-off", adopted from Xu et al., (2019).

In short, the location of reporter molecules above the SERS substrate surface can be adjusted by the conformation change of functional DNAs upon the interaction with metal ions, which enables the feasibility of constructing a SERS metal sensor. Additionally, T-rich, C-rich DNA aptamers and "8-17" DNAzymes show specific binding affinity towards Hg^{2+}, Ag^{+} and Pb^{2+}, which enables the selectivity of using functionalized DNAs as the capturing agent. Many SERS metal sensors have been developed based on reporter location change, especially for Hg^{2+} (Table 3).

Table 3. Reporter locations change based SERS metal sensors.

Metal	Substrate	Reporter	Signal	LOD	Range	Ref
Hg^{2+}	AuNPs/rGO	TAMRA	on	100 pM	N/A	(Ding et al., 2013)
Hg^{2+}	Ag nanorods	Cy5	off	100 fM	1 pM - 1 uM	(Song et al., 2017)
Hg^{2+}	SiO2@Au NPs	oligomer T10G8A8	--	10 nM	10 nM - 1 mM	(Lu et al., 2017)
Hg^{2+}	Au Nanooctahedron Micropinball	TAMRA	on	100 aM	N/A	(Duan et al., 2012)
Hg^{2+}	Au@Ag NPs	Cy3	--	10 pM	10 pM - 1 uM	(Chung et al., 2013)

Hg^{2+}	Ag film	Cy5	on	1.35 fM	10 fM – 1 uM	(Liu et al., 2018)
Hg^{2+}	Au microshell	TAMRA	on	50 nM	N/A	(Han et al., 2010)
Hg^{2+}	AuNPs decorated Si nanowire	Cy5	on	1 pM	1 pM - 100 uM	(Sun et al., 2015)
Pb^{2+}	Fe_3O_4@Au@Ag NPs	Cy3	off	5 pM	10 pM – 1 nM	(Xu et al., 2020)
Pb^{2+}	Au/Ag/Graphene nanostructures	Cy3	on	4.31 pM	10 pM – 100 nM	(He et al., 2021)

2.3.4 Substrate Property Change

The electromagnetic field generated by the SERS substrate is significantly stronger than the SERS signal enhanced from the reporter molecule and thus if the interaction between metal ions and the capturing agent can affect the substrate's properties, the analyte metal ions can be detected by monitoring the reporter molecule's SERS signal change. The substrate's properties can be affected from two aspects, those being the surface physicochemical properties and the substrate concentration. Since SERS is a surface-sensitive technique, changes to the substrate's surface properties can affect both the reporter molecule adsorption and the substrate activity (*e.g.,* electromagnetic enhancement). When increasing the substrate concentration, the distance between adjacent NPs decreases, which can lead to the coupling of the LSPRs of the NPs and result in a stronger electromagnetic enhancement.

2.3.4.1 Substrate Surface Property Change

The surface properties of the SERS substrate can be affected by the formation of an amalgam caused by the reduction reaction between Hg^{2+} and the capturing agent on the substrate surface. This surface impurity can affect the surface plasmon resonance and change the zeta

potential of the SERS substrate. This subsequently attenuates the electromagnetic enhancement and changes the surface charge of the substrate resulting in both the lowered SERS substrate activity and the weakened adsorption of reporter molecules, especially electrostatic-based adsorption (Ren et al., 2012). Therefore, the formation of amalgam on the SERS substrate surface leads to the decreased SERS signals of the reporter molecule, which can be used to construct a "turn-off" SERS sensor. For example, an amalgam shell can form on citrate capped AgNPs surfaces due to complexation and the reduction reaction between the Hg^{2+} and the citrate, where the citrate ions act as the capturing agent (Ren et al., 2012) (as shown in Figure 2.10A). Without Hg^{2+}, the reporter molecule adsorbs on the AgNPs surface via the electrostatic interaction where the citrate ions contribute to the negative charge and the resulting SERS signal. In the presence of Hg^{2+}, the formation of amalgam causes the desorption of citrate ions, resulting the decrease of the zeta potential of the AgNPs, thus leading to the release of the positive charged reporter molecule and a decreased SERS signals (Ren et al., 2012). Similarly, Hg amalgamated on ZnO/Ag nanoarrays can prevent the adsorption of a reporter molecule (*i.e.,* Rhodamine B) (Kandjani et al., 2015). These oxide-based SERS substrates require high temperature stabilities to allow the thermal removal of the adsorbed mercury from the substrate surface following each use (Kandjani et al., 2015). More examples of SERS sensors by using Ag-Hg amalgama based substrate surface property changes can be seen listed in Table 4.

A change in the SERS substrate's surface properties induced by metal ions can also affect the Raman active reporter molecule generation, where the SERS substrate simultaneously participates in the process of reporter molecule generation as the catalyst.

Some SERS-active nanocomposites are used as the SERS substrate while also possessing oxidase-like catalytic activity (Guo et al., 2018; Qi et al., 2015; Song et al., 2020). Plus, some molecules possess higher Raman cross-section when in their oxidized states, such as 3,3',5,5'-tetramethylbenzidine (TMB) that has a poor SERS signal when compared to oxidized TMB (oxTMB) (Ma et al., 2021). Therefore, metal ion-induced surface property changes can simultaneously affect the SERS substrate activity and the generation of the reporter molecules. For example (as shown in Figure 2.10B), hexoctahedral Au nanoparticles can be fabricated with Pt on its edges via silver-mediated temperature-controlled deposition (Au@AgPt NPs), where the AuNPs has the SERS activity, and the Pt shows high catalytic performance for TMB oxidation via a Fenton-like reaction with H_2O_2. Mercaptohexanol (MCH) was functionalized on the Au@AgPt NPs to act as a capturing agent (Song et al., 2020). Hg^{2+} captured by MCH and brought to the substrate surface can react with Pt atoms to produce Pt^{2+} ions and Hg atoms. Because of the consumption of Pt atoms, the Hg^{2+} induced substrate surface property change led to the decreased oxidase-like catalytic activity of the Au@AgPt NPs. Thus, the oxidation-reduction reactions between TMB and H_2O_2 was inhibited, resulting in less generation of Raman active oxTMB, leading to a "turn-off" SERS signals.(Song et al., 2020) Furthermore, because of the blue color of oxTMB, this sensor could also be utilized as a colorimetric sensor. Similarly, Ag-$CoFe_2O_4$/reduced graphene oxide (rGO) nanocomposites have been utilized for Hg^{2+} detection, wherein the Ag-Hg alloy formation on the substrate surface could enhance the catalytic activity of the substrate in the reaction between TMB and dissolved oxygen to generate more oxTMB, thus, resulting in an enhanced SERS signal (Guo et al., 2018).

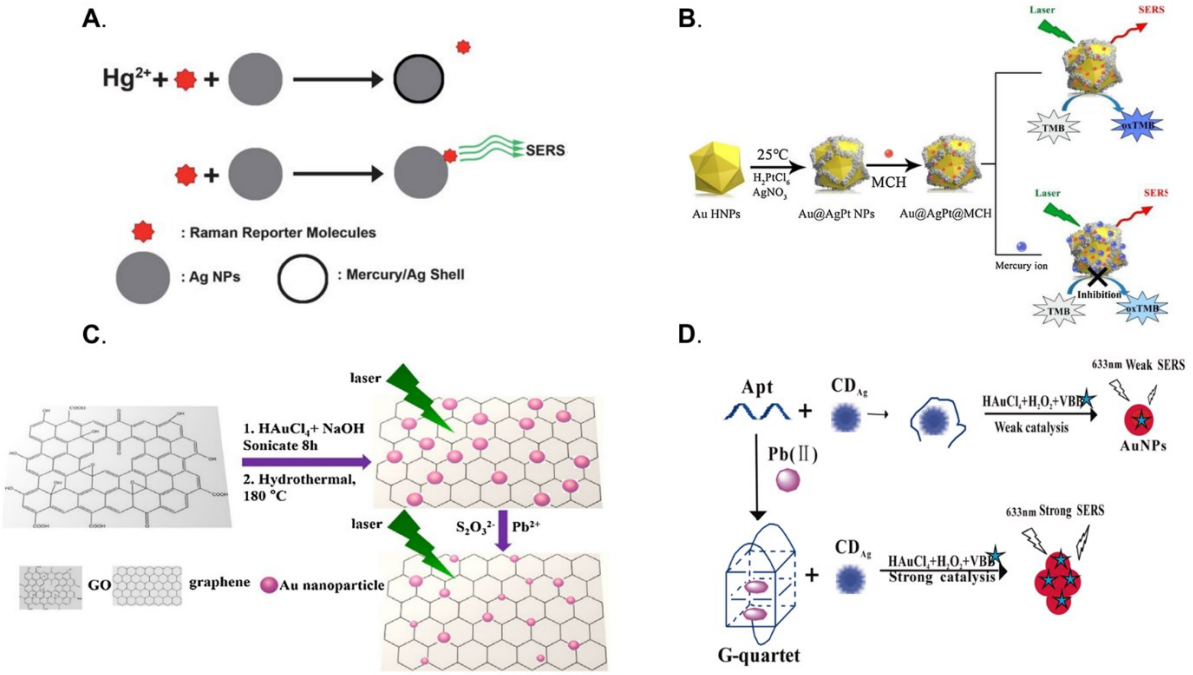

Figure 2.10 SERS metal sensor based on surface property change via (A) Ag-Hg alloy formation, adopted from Ren et al., (2012), (B) substrate catalytic activity, adopted from Song et al., (2020); SERS metal sensor based on substrate concentration change via (C) direct etching, adopted from Zhao et al., (2016); (D) AuNPs generation, adopted from Wang et al., (2019).

2.3.4.2 Substrate Concentration Change

In addition to their effect on the substrate's surface properties, metal ions can also influence the substrate via regulating the concentration of the substrate itself, thus, leading to the SERS signal change of the reporter molecule. The SERS substrate concentration can be regulated by the interaction between metal ions and an etching agent, where metal ions can either inhibit or accelerate the etching rate. For example, thiosulfate ($S_2O_3^{2-}$) can slowly dissolve AuNPs and Au@Ag NPs in aqueous solutions in the presence of dissolved oxygen (Lee & Huang, 2011; Zhu et al., 2018). It has been found that different metal ions can either

accelerate or inhibit the rate of $S_2O_3^{2-}$ etching on NPs (Lee & Huang, 2011; Lou et al., 2011). For example (as shown in Figure 2.10C), Pb^{2+} can act as a catalyst to accelerate the $S_2O_3^{2-}$ etching of AuNPs within the AuNPs/rGO composites, where rGO also acted as the reporter molecule (Zhao et al., 2016). Therefore, in the presence of Pb^{2+}, the concentration of AuNPs decreased, resulting in the less electromagnetic enhancement, therefore leading to a "turn-off" SERS signal of rGO (Zhao et al., 2016). In contrast, Hg^{2+} can interact with $S_2O_3^{2-}$ to form an insoluble substance, HgS, that can protect the SERS substrate (*i.e.,* Au@Ag NPs), from etching, which is also known as an anti-etching process (Wang et al., 2021). Therefore, the increasing concentration of Hg^{2+} can avoid the SERS substrate concentration decrease, allowing the SERS substrate to remain with high activity, and thus, resulting in stronger SERS signals of the reporter molecule (R6G) (Wang et al., 2021). In addition to using etching agents to control the SERS substrate concentration, metal ions can also affect the generation of SERS substrate, subsequently, affecting the SERS substrate concentration.

Metal ions can also affect the activity of the catalyst that catalyze the SERS substrate generation, thus affecting the SERS signals. As an example of this mechanism, the SERS substrate generation based on the $HAuCl_4$ reduction to generate AuNPs, can improve the generation rate, using a proper catalyst such as carbon dot (CD) (Li et al., 2019; Wang et al., 2019; Wang et al., 2021). Therefore, when the target metal ions affect the catalytic activity, the generation of the SERS substrate can be influenced. Ag-doped CD (CD_{Ag}) show an enhanced catalytic activity in the redox reaction between $HAuCl_4$ and H_2O_2. However, the DNA aptamer adsorbed on the CD_{Ag} surface can weaken this catalysis. Therefore, when using metal-specific DNA aptamers, a SERS metal sensor can be constructed. As shown in

Figure 2.10D, a Pb^{2+} specific DNA aptamer adsorbed on the CD_{Ag} surface can inhibit the generation of AgNPs, resulting in poor SERS signal of the reporter molecule (*i.e.,* Victoria blue B; VBB). Because of the high affinity between DNA aptamer and Pb^{2+}, the DNA aptamer is released from the CD_{Ag} surface and instead interacts with Pb^{2+} to form a stable G-quadruplex. Therefore, the catalytic activity of CD_{Ag} was recovered, which accelerated the AuNPs generation and produced a stronger SERS signal (Wang et al., 2019). Similarly, in addition to different CDs, AuNPs, silver-doped carbon nitride quantum dots (AgCNs), and graphene oxide nanoribbons have also been utilized as catalysts in AuNPs generation, and by using different metal specific binding DNA aptamers, SERS sensor for different metal ions detection have been constructed (Li et al., 2018, 2020; Ouyang et al., 2018; Ye et al., 2016). More examples of metal ions detected by substrate property change has been listed in Table 4.

Table 4. SERS metal sensors based on substrate property change.

Metal	Substrate	Reporter	Signal	LOD	Range	Ref
Hg^{2+}	AgNPs	Crystal violet (CV)	off	90.9 pM	N/A	(Ren et al., 2012)
Hg^{2+}	AgNPs	acriflavine	off	1.4 nM	4.7 nM – 80 nM	(Hao et al., 2020)
Hg^{2+}	AgNPs	MB	off	100 nM	N/A	(Yan et al., 2019)
Hg^{2+}	AgNPs	4-MPY	off	340 pM	1 nM – 100 nM	(Chen et al., 2014)
Hg^{2+}	AuNPs	CV	off	500 fM	500 pM – 5 nM	(Fu et al., 2014)
Hg^{2+}	ZnO/Ag	RB	off	2.24 pM	N/A	(Kandjani et al., 2015)
Hg^{2+}	Fe_3O_4@SiO_2-Au	Congo red	off	10 nM	10 nM – 100 uM	(Sun, et al., 2016)

Hg^{2+}	Ag-$CoFe_2O_4$	oxTMB	on	670 pM	2 nM – 10 nM	(Guo et al., 2018)
Hg^{2+}	Au@AgPt NPs	oxTMB	off	280 pM	1 nM – 10 uM	(Song et al., 2020)
Hg^{2+}	AgNPs	DAP	on	1 nM	1 nM – 10 uM	(Qi et al., 2015)
Hg^{2+}	Au-NiFe LDH/rGO	oxTMB	on	10 nM	10 nM – 100 nM	(Liu et al., 2021)
Hg^{2+}	AuNBs	4-MBA	off	50 nM	100 nM – 10 uM	(Qi et al., 2018)
Pb^{2+}	AuNPs/rGO	rGO	off	1 nM	5 nM – 4uM	(Zhao et al., 2016)
Hg^{2+}	Au@Ag NPs	R6G	on	100 pM	100 pM – 1uM	(Wang et al., 2021)
Hg^{2+}	AgNPs	pATP	off	2 nM	4 nM – 350 nM	(Kang et al., 2017)
Co^{2+}	AuNPs	VB4R	on	20 pM	33 pM – 1 nM	(Wen et al., 2021)
Hg^{2+}	AuNSs	4-MBA	off	50 pM	100 pM – 100 uM	(Chen et al., 2018)
Hg^{2+}	AuNPs	4-MBA	off	30 pM	100 pM – 1 uM	(Yang et al., 2020)
Pb^{2+}	AuNPs	VBB	on	70 pM	130 pM – 53.33 nM	(Ouyang et al., 2018)
Na^{+}	AuNPs	VB4r	on	1.9 nM	4 nM – 0.043 nM	(Li et al., 2019)
K^{+}	AuNPs	VBB	on	920 pM	5 nM – 150 nM	(Li et al., 2020)
Pb^{2+}	AuNPs	VBB	on	3.2 nM	6 nM – 460 nM	(Wang et al., 2019)
Pb^{2+}	AuNPs	VBB	On	1 nM	17 nM – 250 nM	(Ye et al., 2016)
Pb^{2+}	AuNPs	VBB	on	700 pM	2 nM – 75 nM	(Li et al., 2018)

2.4 Sensitivity of the SERS Metal Sensors

Sensitivity is another important feature of an analytical tool for metal ion detection. Ultrasensitive sensors are needed for identification and monitoring of metal ions that can represent a risk even at very low concentrations in the environment (Arjomandi & Shirkhanloo, 2019). To achieve the highest sensitivity of a SERS metal sensor, three aspects must be taken into consideration, which are (1) optimizing the reaction conditions, including the ideal SERS substrate; (2) choosing effective signal amplification strategies and (3) using proper pretreatment method.

2.4.1 Ideal SERS Substrate

The SERS substrate usually determines the dominant SERS effect since it is the place that generate the signal. In addition, as introduced in previous enhancement mechanism discussion above, the SERS substrate can both contribute to the electromagnetic and chemical enhancements. Electromagnetic enhancement tends to dominate in SERS enhancement mechanisms, where the enhanced electromagnetic field is generated by surface plasmon resonance of SERS substrate under the incident light excitation. Therefore, the SERS substrate plays an important role in the SERS sensitivity. However, based on the different signal generation mechanisms, SERS substrates with different sizes, morphologies, configurations, and components can contribute differently to the sensitivity of the SERS metal sensors. Therefore, an optimized SERS substrate is necessary to achieve the maximum enhancement.

SERS substrates with different morphologies shows different electromagnetic enhancement. Compared to spherical nanoparticles, anisotropic nanostructures, such as Au nanostars, can offer higher electromagnetic enhancement since it can couple the electromagnetic field generated at the core, corner, and tips. In addition, when using anisotropic nanoparticles in inter-substrate distance change-based SERS metal sensors, the nanogap between the tips of the substrate can generate strong electromagnetic enhancement, thus the reporter molecule located in the nanogap generates more intensive SERS signals (Ma et al., 2013; Ndokoye et al., 2014).

The SERS substrate configuration can be simply classified into two types that are colloidal nanoparticles and the solid nanostructured nanomaterials. When using reporter molecular recognition mechanisms, the SERS substrate with a solid nanostructure is preferred since its well-ordered structure can provide sufficient hot spots that can offer a uniform electromagnetic enhancement. As such, these NPs can have more intense SERS signals comparing to using dispersed colloidal nanoparticles. In contrast, when using inter-substrate distance change, colloidal nanoparticles are preferred over solid nanostructure material, since with the interaction with metal ions, the distance between colloidal nanoparticles could be easily changed.

The substrate size is important when utilized in substrate concentration- based metal ion detectors. For example, when using AuNPs as the catalyst to generate more SERS substrate, the size of AuNPs showed different catalytic performance (Ouyang et al., 2018).. It has been found that smaller size NPs have the higher catalytic performance, since small

nanoparticles have large surface area and more surface electrons available for redox reactions. In addition, using smaller AuNPs can achieve a lower Pb^{2+} detection (Ouyang et al., 2018).

The SERS substrate based on Au/Ag based nanocomposites have different advantages contributing to the sensitivity based on different applications. For example, graphene-based nanocomposites have been widely used as SERS substrate because graphene quenches the fluorescence signals thereby improving the SERS signal quality, but also contributes to the chemical enhancement because of the easier charge transfer between the reporter molecules and the SERS substrate (Annavaram et al., 2019; Tao & Wang, 2018). In addition, magnetic SERS substrate not only have better electromagnetic enhancement comparing to rare Ag or Au nanoparticles, but also can be easily collected with a magnet for sample enrichment, which can help to eliminate the matrix effect from environmental samples when doing the SERS measurements (Yang et al., 2017).

In addition to using the proper SERS substrate, choosing an effective signal amplification strategy can further improve the sensitivity of the SERS metal sensors.

2.4.2 Effective Signal Amplification Strategy

In addition to using appropriate SERS substrate, some signal amplification strategies can also help to further increase the sensitivity of SERS metal sensors. Firstly, since the electromagnetic field is generated by the surface plasmon resonance that is induced by the interaction of incident light and the SERS substrate, the laser wavelength used to excite the substrate also affects the electromagnetic enhancement. However, depending on the different signal generation mechanisms, the substrate state can change, which may affect their surface plasmon. For example, using inter-substrate distance change-based mechanism, the LSPR

will be different before and after the interaction with metal ions. Therefore, choosing optimal laser wavelengths to excite the SERS substrate is important. When the laser wavelength is in the resonance of the LSPR of the SERS substrate, greater electromagnetic enhancement can be expected.

2.4.3 Pretreatment Methods

Pre-treatment of samples is widely used in analytical chemistry to isolate or concentrate the analyte of interest. Typical sample preconcentration applied in order to increase the sensitivity in metal ions by SERS can be divided into three types: (1) centrifugation, (2) evaporation (drop and dry) and (3) magnetic separation. Firstly, the simplest way of preconcentration is use of a centrifuge followed by the redispersion of the sample pellet into a smaller volume of the appropriate medium. Centrifugation can be used to enrich not only the analyte but also the SERS substrate, which contributes to a better sensitivity of the SERS measurement. The evaporation method is often used to enrich the analyte at the laser spot, such that the analyte concentration and signal intensity will be increased, improving the sensitivity of the sensor. By using a magnetic SERS substrate, a magnet can be used, and the adsorbed reporter molecule can be collected and concentrated. In addition, magnetically concentrated SERS substrates can form sufficient hot spots, as substrate can be tightly collected, which can dramatically enhance the SERS signals of reporter molecules, resulting in improved sensitivity.

2.5 Quantitative Analysis of SERS Metal Sensors

It is worth to note that the SERS signal reproducibility of the substrate plays a fundamental role in quantitative analysis. For example, when using reporter molecular recognition mechanism, it is important for substrate to provide stable SERS signals before and after with the metal ions interaction. If the SERS substrate experience the unexpected aggregation during the SERS measurement, the SERS signals will be dramatically enhanced, which cannot be trustable and used for quantitative analysis. Therefore, in this case, it is preferred to use solid nanostructured substrate with well-ordered assemble, which can prove reproducible and stable SERS signals.

Before the quantitative analysis of metal ions, it is important to identify the SERS spectrum change caused by metal ions. According to the SERS signal generation mechanism mentioned above, the metal ions can be identified in three different ways, which are based on (1) peak shift, (2) new peak generation and (3) peak intensity variation of the SERS spectrum of the Raman reporter molecule. After confirming that the SERS spectrum change is indeed caused by target metal ions, the peak selection is another key consideration. If the SERS spectrum change is based on peak shift and new peak generation, usually the shifted or new peak is utilized as the characteristic peak for quantitative study of the metal ions, which is usually used for the molecular recognition-based mechanism. If the SERS spectrum change is based on the shole spectrum intensity change, the most intensive peak of the reporter molecule is usually used for quantitative analysis, since the most intensive peak represents the most sensitive vibrational mode.

After selecting the characteristic peak, the intensity change of that peak is usually used to do the quantitative analysis. In order to avoid the affect from the substrate stability, laser stability and the measurement environment, different internal standards can be choose based on the different signal generation mechanism. For example, when using molecular recognition mechanism, some build-in internal standards can be used. The reporter molecule usually has different moieties. The metal binding site has the altered spectral features upon the complexation with metal ions, however, other functional groups remain the same, which can be used as a build-in internal standard. When using the reporter location change based mechanism, an extra reporter molecule is needed as the internal standards, since by changing the location of the reporter molecule, the overall intensity of SERS spectrum is changed. For example, p-aminothiophenol (pATP) was used as internal standard in DNA aptamer-based reporter molecule location changed SERS platform. The SERS signals change of pATP represents the system instability, but by using the radiometric quantitation, the SERS platform can be accurate and used for quantitative analysis (Shi et al., 2018).

2.6 Current Limitations and Future Opportunities

Research on the use of SERS for metal ions detection has made remarkable recent achievement, including the development of diverse sensing methods, high sensitivity, and the potential for real sample applications. However, in order to become an accurate, highly sensitive, and selective quantitative analytical tool current SERS metal sensors still face some challenges and limitations. These current limitations arise from our limited understanding of the fundamental principles that are the basis behind the building SERS bases sensors. Since SERS is a form of molecular spectroscopy, the detection of atomic metal

ions using SERS technology is an indirect approach, relying on spectra alterations resulting from the interaction between metal ions and the reporter molecules. These emerging SERS metal sensors are therefore more complex relative to traditional SERS sensors that detect the analyte directly.

To achieve reliable quantitative metal ion analysis, it is critical but challenging to have good quality control of the SERS substrate. As discussed above, both signal generation mechanisms (*i.e.,* inter-substrate distance change and the substrate concentration change) involve metal ion induced SERS substrate change, so the colloidal stability of the SERS substrate plays a key role. However, the control of substrate aggregation is difficult, especially when colloidal substrates are under a high-ionic environment, and may suffer from non-specific aggregation, preventing the SERS metal sensor from real sample detection. In addition, the instability of the SERS substate also contributes to the fluctuation of SERS signals which decreases the quantitative capability of SERS metal sensors.

The ability to apply assays for multiple metal ions (multiplex) using current reporter molecular recognition-based SERS metal sensors remains a challenge. Using a single reporter molecule to detect multiple metal ions could greatly benefit the SERS metal sensor applications. With a portable Raman spectroscopy, a multiplexed SERS sensor will be ideal for remote and on-site analysis. Even though some reporter molecules possess a functional group that can coordinate with different metal ions, the competition for binding of different metal ions is unavoidable, which leads to poor quantitative capability of the multiplexed SERS metal sensors. Although engineered reporter molecules with multiple functional groups can be used for different metal-coordination currently, the selective interaction

mechanisms between the metal ions and the binding sites remain unclear (Guselnikova et al., 2017). Engineered reporter molecules also require complex synthesis process, which limits large-scale application. Furthermore, pH can strongly affect the coordination reaction, which may affect the interaction between the reporter molecule and the target metal ions, leading to the decreased effectiveness of the SERS metal sensors.

Quantitative aspects of SERS metal sensors still need to improve in both reproducibility and the selectivity. The limited reproducibility comes from the signal repeatability of the SERS substrate and the inter-lab diversification that involves differences in instruments and operation (Fornasaro et al., 2020) Again, since SERS metal sensors are based on the SERS signal intensity change of the reporter molecule the stable electromagnetic enhancement generated by SERS substrate is related to having a stable SERS signal of the reporter molecule. Therefore, the uniformity of the SERS substrate can strongly affect the repeatability of the SERS signals. However, even if the SERS substrate remains uniform, with different instruments and operations the repeatability of the SERS metal sensors can be affected. For example, using different laser excitations, the electromagnetic field generated by the same SERS substrate varies, thus affecting the sensitivity of the SERS metal sensor. For reporter molecule location change based SERS metal sensors, even when the reporter molecule is located at the same position, the different intensity of the electromagnetic field, results in the reporter molecule giving a SERS signals with different intensity, thus affecting the reproducibility of the SERS metal sensors. Both anions and cations may also affect the binding behavior between the target metal ions and the reporter molecules (or capturing agent) thereby affecting selectivity. Thus, maintaining the

high selectivity of the reporter molecules (or capturing agent) remains challenging. Currently, masking agents are commonly used to prevent non-target binding, however, this limits the potential of SERS metal sensor for real sample detection.

Finally, detection of metal ions in real environmental samples using SERS metal sensors remains a major challenge due to inherent matrix effects. For example, organic compounds in environmental samples can generate SERS signals that overlap with the spectral region of the reporter molecules. In addition, particles in the samples can also affect the interaction between the light excitation source and the SERS substrate, altering the electromagnetic enhancement induced by the SERS substrate, thus impacting the accuracy of the SERS metal sensors.

There are many opportunities for SERS researchers to address the remaining issues and develop practical and useful metal sensors. Firstly, it is important to improve our understanding of the basic physiochemical mechanisms that govern the behaviors (*e.g.,* dispersion and aggregation) of nano-substrates, reporter-metal interactions on nanosurfaces, signal generation and amplification in the sensor design. There is a need to continue to improve the engineering and control of the SERS substrate. It is also important to explore and improve the reporter molecule selectivity towards the target metal ions. In addition, improved calibration methods are needed to optimize detection, including innovative approaches for introducing internal standards into the sensor design in order to correct for various matrix effects and improve the sensor capability for quantitative analysis of environmental samples.

Chapter 3
Solvent Effect on Surface Enhanced Raman Spectroscopy

3.1 Introduction

Surface enhanced Raman spectroscopy (SERS) is a promising analytical tool with high specificity and sensitivity which has been widely utilized for environmental monitoring and chemical sensing (Cialla et al., 2012). Compared to conventional, chromatography-mass spectrometry-based methods, SERS can be used for on-site analysis because of its portable nature, cost-effectiveness, and rapid throughput. In environmental analysis, the use of organic solvents play an important role as they have always been used for sample preparation, such as during the liquid extraction of pharmaceuticals (Alpendurada, 2000; Fitzpatrick & Dean, 2002). Thus far, several groups have reported SERS detection in some common organic solvents including ethanol and chloroform. However, in these cases the organic solvent was evaporated prior to the SERS measurement and the analyte was detected on the surfaces of dried substrate film, meaning the analyte was not actually detected in the liquid phase itself (Yang et al., 2016; Yilmaz et al., 2017).

Over the past 4 decades, the theory of SERS signal enhancement (*i.e.,* electromagnetic (EM) enhancement and electrochemical enhancement) has been well documented. The interaction between the metal nanoparticles and the surrounding environment can be modeled based on different parameters, however, there is lack of strong experimental evidence to support many of their conclusions. In particular, the influence of the solvent on SERS detection has not yet been systematically investigated. While some researchers have explored how different solvents may compete for adsorption sites on

colloidal silver surfaces, these experiments were primarily conducted with similar aqueous solutions as opposed to non-polar organic solvents (Rupérez & Laserna, 1994). The rapid and reliable SERS detection method in organic solvents, especially those solvent immiscible with water, is still highly desirable, especially for environmental analysis. In addition, a better understanding of the solvent effect on SERS detection can help to develop a deeper understanding of SERS mechanism and may open many new opportunities for improved sensors.

The objective of this study was to (1) systematically investigate the solvent effect on SERS detection based on the experimental performance and computational modeling, and (2) to develop a rapid and reliable SERS method that could directly detect organic molecules in different organic solvents.

3.2 Materials and Methods

3.2.1 Materials

Silver nitrate ($AgNO_3$, 99.9%), sodium borohydride ($NaBH_4$, 99%), trisodium citrate (99%), 4-aminothiophenol (pATP, 97%) were purchased from Sigma-Aldrich (Oakville, ON, Canada). Anhydrous ethanol (EtOH) and hydrogen peroxide (H_2O_2, 30 wt%) were purchased from VWR (Mississauga, ON, Canada). Methylene chloride (CH_2Cl_2), Chloroform ($CHCl_3$), 2-propanol (97%) were purchased from Sigma (Oakville, ON, Canada). All reagents were used without further purification. Nanopure water (18 MΩ cm) obtained from a Barnstead Nanopure system (Thermo Fisher Scientific, Waltham, MA, USA) and was used in all experiments.

3.2.2 Apparatus

The SERS substrates were analyzed for their optical characteristics, size, and surface charge using UV-Vis spectroscopy, dynamic light scattering (DLS), and zeta-potential measurements, respectively. Transmission electron microscopy (TEM) imaging of the SERS substrates was conducted by collaborators at Acadia University (Wolfville, NS). A portable Surface-Enhanced Raman Spectroscopy system was developed in-house to record the sample spectrum, wherein a solid-state Nd-YAG laser centered at 785 nm was used as the excitation light resource (Figure 3.1). The laser, operating at a power of 450 mW/cm^2, with a beam diameter of 2.5 μm, was introduced to the sample in a cuvette kept in the sample holder using the fiberoptic cable. The laser power at the sample was measured by a Thorlabs PM 100 optical power meter, which was determined as 5 mW/cm^2. The scattered light was collected at 180° by a standard Sunshine TG-Raman fibre spectrometer (Changchun New Industries Optoelectronics Tech. Co., Ltd., Changchun, China). The signal integration time for each sample was fixed at 500 ms to obtain the spectrum. All samples were measured in triplicate but presented as an average of three measurements.

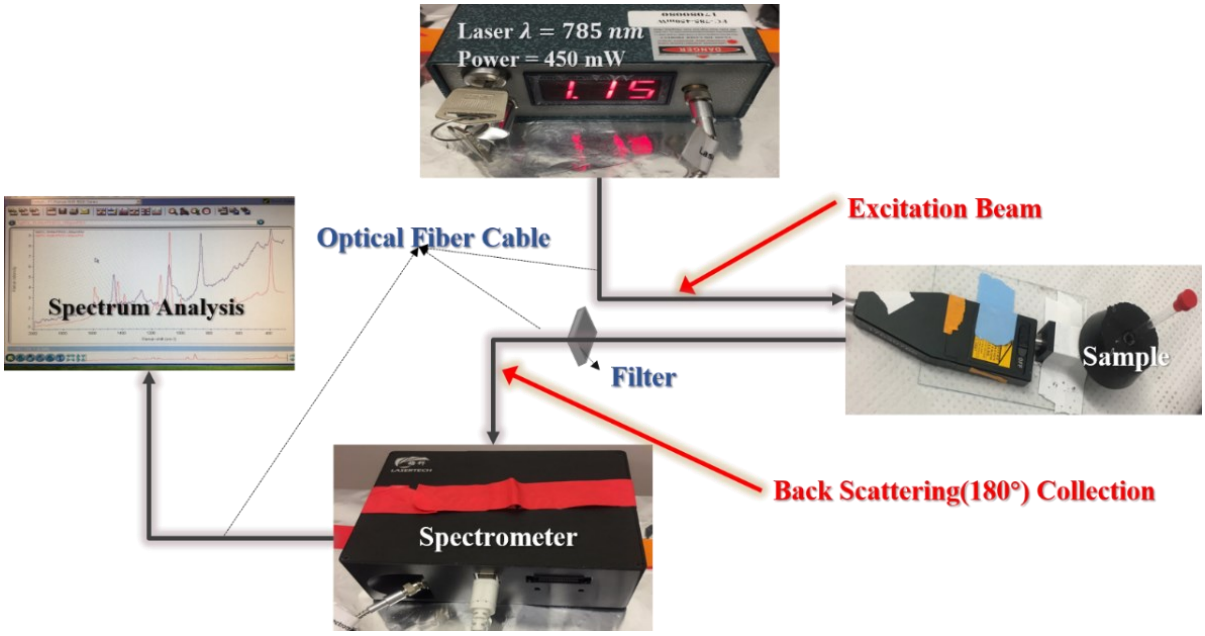

Figure 3.1 SERS experiment setup.

3.2.3 Silver Nanoplate Synthesis (AgNPs)

A modified chemical reduction method was employed to synthesize AgNPs (Zhang et al., 2011). Briefly, 500 µL of aqueous silver nitrate ($AgNO_3$, 0.05M), 5 mL of trisodium citrate (75 mM), 1 mL of ethanol (17.5 mM), 600 µL of hydrogen peroxide (30 wt%), and 241.4 mL of nanopure water were mixed in a 500 mL flask followed by the rapid addition of 1.5 mL sodium borohydride (100 mM) to form AgNPs. The total reaction volume for one synthesis was fixed at 250 mL. The reaction solution was vigorously stirred at room temperature by a magnetic stir bar at 1200 rpm. In the presence of the capping ligand, trisodium citrate, and the secondary ligand, ethanol, sodium borohydride reduced the silver ions to form silver nanoparticles, leading to a color change from transparent to light-yellow in the reaction solution. Over the next 3 minutes, the color of the reaction solution continued to change from light-yellow to blue, indicating the conversion of the silver nanoparticles to nanoplates

induced by hydrogen peroxide. The concentration of the as-synthesized AgNPs was 0.3 nM. The AgNPs was firstly concentrated to 7 nM by centrifugation (12700 RPM, 30 minutes) at 4℃. The concentrated AgNPs was kept in the fridge for future use.

3.2.4 Phase Transfer of AgNPs into Organic Solvents

The concentrated AgNPs were washed with anhydrous ethanol to remove any remaining ions or water residue (Kulkarni et al., 2009). To transfer the synthesized AgNPs into an organic phase, equal volumes (300 μL) of AgNPs and anhydrous ethanol was mixed and sonicated for 5 minutes followed by centrifugation at 12,700 RPM for 1 hour (4°C). After washing the AgNPs with ethanol three times, the pellets were collected and resuspended into different organic solvents that were miscible with ethanol, such as acetone, methylene chloride and chloroform etc., Sonication (up to 5 minutes) was used to assist in fully dispersing the nanoparticle colloid.

3.2.5 Sample Preparation

Serial dilution was used to prepare different concentrations of analyte (pATP) in different organic solvents. Briefly, 12.5 mg of pATP was dissolved in 10 mL of anhydrous ethanol with vortex mixing and ultrasonication to obtain a stock solution of 10 mM.. The pATP stock was diluted with different organic solvents (*e.g.,* ethanol, methylene chloride and chloroform) to prepare different concentrations of pATP in different organic solvents. A series of 100-fold dilutions (20 μL into 1 mL) was used for all sample preparation, which maintain 1% ethanol in all organic solvents with pATP dissolved.

3.2.6 SERS Detection in Organic Solvents

AgNPs dispersed in different organic solvents (150 μL) were mixed with an equal volume of pATP solution and mixed by vortex mixing and ultrasonication to allow adsorption on the AgNPs surface. All SERS measurements were operated in 5 x 100 mm quartz NMR tubes (0.5 mm quartz thickness). The integration time for each sample was fixed at 500 ms to obtain the spectrum. All samples were measured in triplicate and the spectra presented as an average of the three measurements.

3.2.7 Computation of the Electric Field Enhancement of Surface Plasmons

According to the TEM images, a model of the nanoparticle aggregates was modeled in Metlab and the electromagnetic field (E-Field) enhancement of the surface plasmons was modeled utilizing the boundary element method (BEM) approach for different aqueous and organic solvents as previously described in the literature (Abajo & Howie, 1998, 2002; Hohenester & Krenn, 2005; Lagos et al., 2017).

3.3 Result and Discussion

3.3.1 Characterization of AgNPs

The AgNPs were synthesized based on the redox reaction between $AgNO_3$ and $NaBH_4$, where citrate and ethanol were used as capping ligands to stabilize the AgNPs and H_2O_2 helped with the conversion of the silver nanoparticles into nanoplates. The primary morphology of the AgNPs was a triangular shape with a smaller number of spherical particles as revealed by TEM imaging (Figures 3.2A and 3.2B). The average diameter of the

AgNPs was determined as ~17 nm by the TEM imaging and the size distribution of AgNPs can be seen in Figure 3.2C. In addition, UV-Vis absorption spectroscopy showed the synthesized AgNPs possessed the main plasmon resonance peak around 650 nm, as shown in Figure 3.2D.

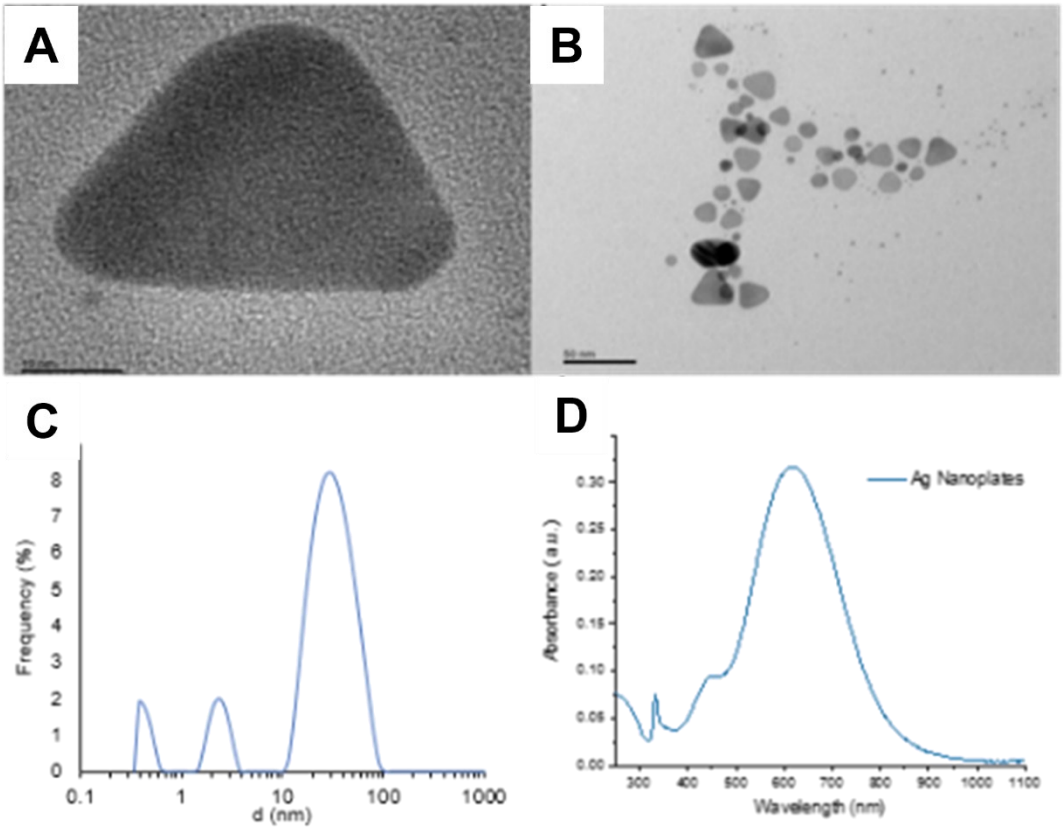

Figure 3.2 (A) and (B) TEM image; (C) size distribution; (D) UV-Vis spectra of AgNPs

3.3.2 SERS Detection in Organic Solvents

3.3.2.1 Phase Transfer of SERS substrate

In order to take SERS measurements in organic solvents, the AgNPs synthesized in water first needed to be transferred into different organic solvents themselves. The phase transfer of

AgNPs involved two steps, wherein the AgNPs were first transferred into ethanol before being transferred into organic solvents that were miscible with ethanol (Figure 3.3). During synthesis, ethanol was used as the secondary capping ligand with a lower concentration than citrate. By washing several times with ethanol, the remaining water molecules and the loosely bound citrate ions were replaced by ethanol, increasing the hydrophobicity of the AgNPs were dramatically. Since the organic solvents used here were miscible with ethanol, the ethanol-AgNPs were able to be readily transferred into the organic phase.

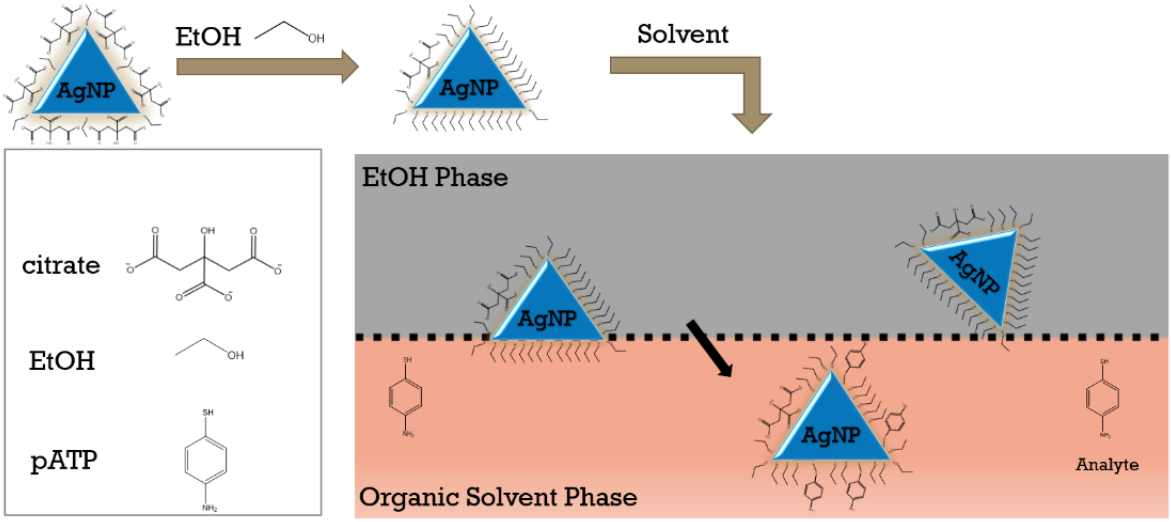

Figure 3.3 Phase transfer mechanism of AgNPs from aqueous to organic solvent

When the analyte, pATP, was dissolved in organic solvents, pATP could easily adsorb on the AgNPs surface via Ag-S covalent bonds. Because of the adsorption of pATP, the repulsion force between adjacent AgNPs was decreased and aggregation was induced. In the resulting nanoaggregates, nanogaps (*i.e.,* hot spots) capable of plasmon-plasmon coupling were formed, wherein the surface adsorbed pATP molecules are exposed to the highest electromagnetic field and produce the strongest SERS signal.

3.3.2.2 Detection of pATP in Methylene Chloride

Unlike water molecules, organic solvent molecules have Raman signatures which can overlap with the analyte spectra. Therefore, in order to successfully utilize SERS detection in organic solvents, the Raman signals of the analyte should have at least one characteristic peak that doesn't overlap with the solvent being used. When methylene chloride was employed as the solvent, the spectra of pATP showed three main vibrational modes within the window of 1000-1700 cm^{-1} (Figure 3.4). Compared to the Raman spectrum of methylene chloride, the =C-S and C=C vibrational modes, located between 1070-1080 cm^{-1} and 1570-1580 cm^{-1} respectively, could be used as the characteristic pATP peaks for SERS detection. In contrast, the C-H bending (1135-1142 cm^{-1}) of pATP was overlapped with the CH_2 twist of methylene chloride, and thus could not be used for pATP identification.

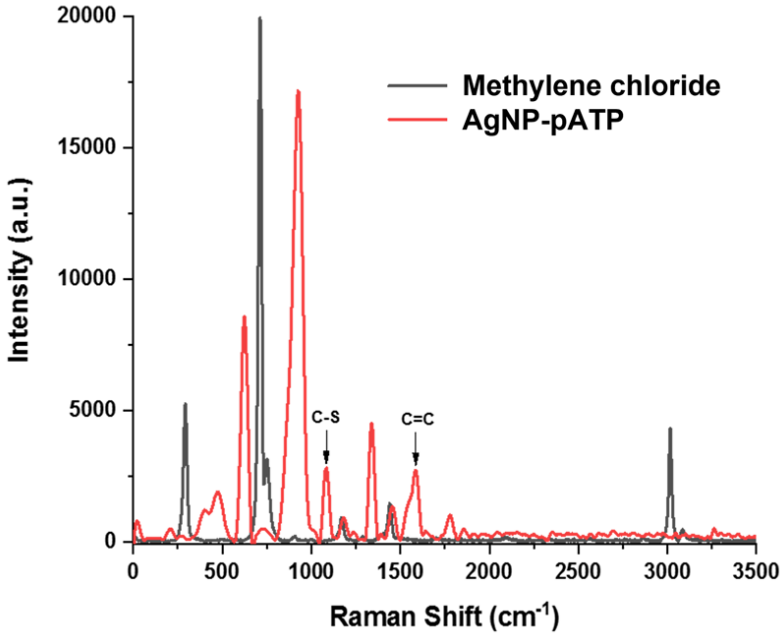

Figure 3.4 Raman spectrum of methylene chloride (black) and SERS spectrum of pATP, where AgNPs used as substrate (red).

With such characteristic peaks identified, SERS detection of pATP with AgNPs as the substrate was conducted in methylene chloride (Figure 3.5). The SERS spectrum of pATP in methylene chloride showed that the C-S, C-H and C=C vibrational modes could be obtained, whereas the control group, which only contained AgNPs, did not show any significant peaks between 1000-1700 cm^{-1}.

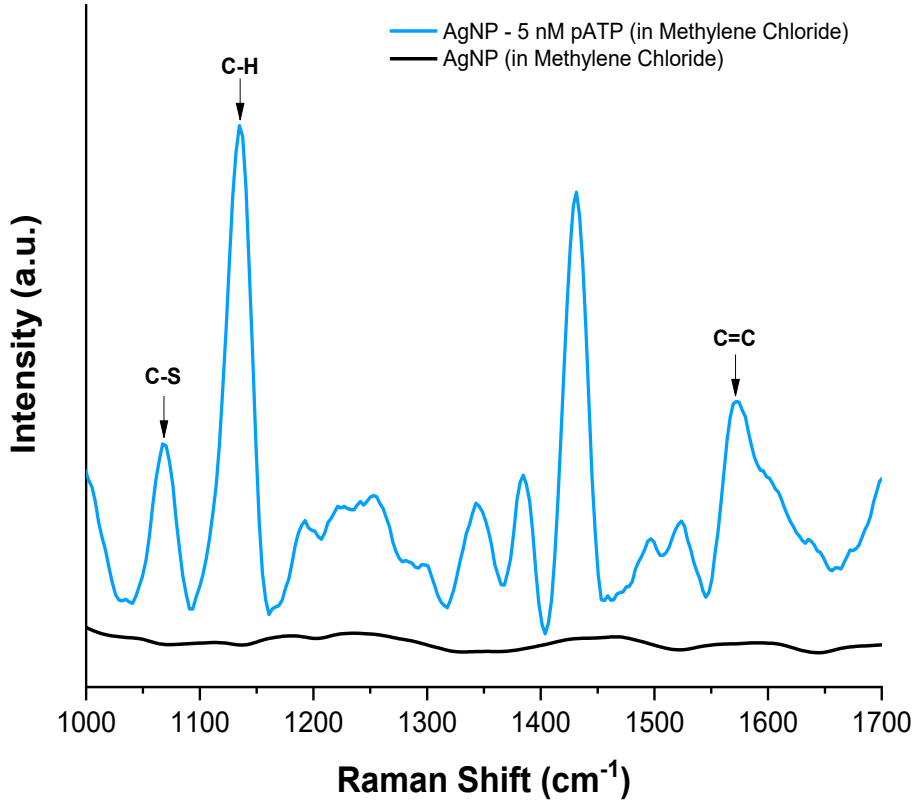

Figure 3.5 The SERS spectrum of 5 nM pATP in methylene chloride

3.3.3 Ultrahigh Sensitivity of SERS Detection in Organic Solvents

Based on the SERS detection in organic solvents, the limit of detection (LOD) of pATP was studied. Surprisingly, ultrahigh SERS sensitivity was achieved in methylene chloride (Figure

3.6), where the LOD pATP was determined as 5 zM. Even at zM level, the vibrational mode of C-S and C=C of pATP was clearly observed in the spectrum.

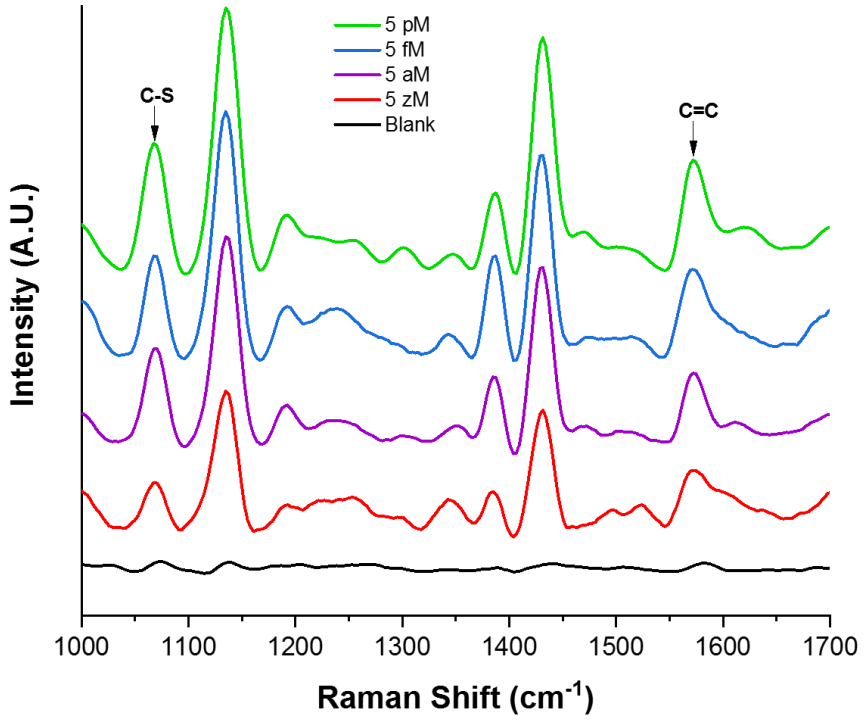

Figure 3.6 Different concentrations of pATP detected by SERS in methylene chloride.

Careful detection of pATP was also performed in ethanol, chloroform, and nanopure water solutions. Similar to methylene chloride, the sensitivity of the SERS detection in chloroform was ultrahigh, wherein the LOD of pATP was 1 aM. However, the LOD of pATP in ethanol and water were only found to be at the pM and nM level respectively. Comparing to water, the LOD of pATP in organic solvent was significantly lower, which showed the higher sensitivity of SERS detection in organic solvents. The correlation of the LODs of pATP in different solvents and the dielectric constant of the solvents were illustrated in Figure 3.7, which showed a general trend of lower dielectric media producing higher SERS

sensitivity. When comparing chloroform and water, where the dielectric constant of chloroform is roughly 15 times lower than that of water, the SERS detection of pATP in chloroform showed ultra-high sensitivity and fulfilled the trend. However, when the difference in dielectric constant was small, such as with chloroform and methylene chloride the LOD decreased with the dielectric constant. However, compared to ethanol and water, the LOD of pATP in chloroform was still at aM level, which was still ultra-sensitive.

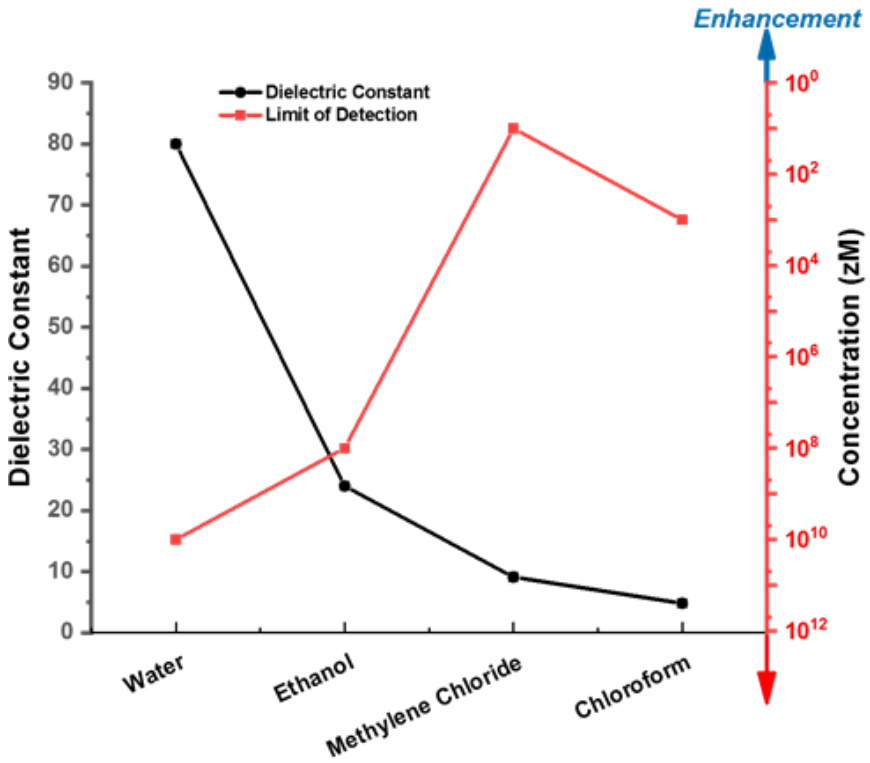

Figure 3.7 The dielectric constant and the SERS Limit of Detection (LOD) of different solvents

3.3.4 Theoretical Considerations and Computational Modeling

In order to better understand the ultra-sensitivity of SERS detection in organic solvents, the different enhancement mechanisms have been reviewed (Rojas & Claro, 1993). It is well

known that both electromagnetic and chemical enhancement can contribute to the Raman signal of molecules on metal nanoparticles, with the electromagnetic enhancement typically being the dominant enhancement mechanism. The electromagnetic enhancement of the SERS signal is governed by the localized surface plasmon of the metal nanoparticles. When the AgNPs are irradiated by an external electromagnetic wave (E_0), the conduction and valence electrons on the AgNPs surface will be excited. Since the average size of AgNPs is 17 nm and is much smaller than the 785 nm of laser wavelength, the electric field around AgNPs is considered uniform. The excited surface electrons oscillate collectively at the interface of metal nanoparticles and the surrounding solvent. This surface plasmon excitation induces a dipole moment, inducing elastic scattering at the same frequency (ω) of the external electromagnetic wave. Therefore, the local field (E_L) on the AgNP surface affecting the adsorbed molecule (pATP) is a coupled field resulting from both the external electromagnetic wave (E_0) and elastic scattering generated by surface plasmons on the AgNPs (Eq. 1), where g_1 is the enhancement factor of the local field.

$$E_L(\omega) = g_1(\omega)E_0 \quad \text{(Eq. 1)}$$

The adsorbed molecule (pAPT) is excited by the local field (E_L). The induced dipole moment of the molecule (p_m), see Eq. 2, then generates a field ($\widetilde{E}_L$) at a different frequency (ω_R) compared to the local field via Raman scattering. This field ($\widetilde{E}_L$) at frequency ω_R further induces another dipole moment (p_{AgNP}) in the AgNPs as shown in Eq 3., thus generating another field (E_R) at the same frequency (ω_R). This field (E_R) is related to the field $\widetilde{E}_L$ and is affected by the enhancement factor g_2. The α_m and α_{AgNP} represent the polarizability of the adsorbed molecule and silver nanoparticle, respectively.

$$p_m(\omega_R) = \alpha_m(\omega_R, \omega)E_L(\omega) \quad \text{(Eq. 2)}$$

$$p_{AgNP}(\omega_R) = \alpha_{AgNP}(\omega_R)\tilde{E}_L(\omega_R) \quad \text{(Eq. 3)}$$

Therefore, the produced SERS signal is the total dipole moment (p) at the molecule and the AgNPs at the frequency ω_R, written as Eq. 4.

$$p(\omega_R) = g_1(\omega)g_2(\omega_R)\alpha_m(\omega_R, \omega)E_0 \quad \text{(Eq. 4)}$$

The intensity of the radiation field is proportional to the square of the total dipole moment, therefore the enhancement (Q) of SERS signal comparing to normal Raman signal is the square of the absolute value of the product of g_1 and g_2, see Eq. 5.

$$Q = |g_1(\omega)g_2(\omega_R)|^2 \quad \text{(Eq. 5)}$$

From the above discussion, it is clear that the dominant electromagnetic enhancement of SERS is related to the enhancement factor g_1 and g_2 and the simplified determination of g is presented in Eq. 6 (Stiles et al., 2008).

$$g = \frac{\varepsilon_{AgNP} - \varepsilon_{solvent}}{(\varepsilon_{AgNP} + 2\varepsilon_{solvent})} \quad \text{(Eq. 6)}$$

Here ε_{AgNP} represents the dielectric constant of the AgNPs and $\varepsilon_{solvent}$ is the dielectric constant of the surrounding media. When using the same AgNPs but with a different solvent the enhancement factor varies. Notably, when the solvent has a lower dielectric constant, theoretically, the enhancement factor should also increase. Thus, the SERS signal should be increased dramatically since the SERS enhancement is roughly 10^4 higher compared to the solvent with higher dielectric constant.

Our experimental results agree with the general electromagnetic enhancement theory. However, our results show also indicate a 10^4 higher enhancement than predicted. One

reason for this may be the formation of hot spots which can dramatically promote the electromagnetic enhancement even further through plasmon-plasmon coupling.

To examine how the difference in dielectric constants of the solvents could dramatically affect the electromagnetic enhancement of SERS performance, we stimulated the plasmonic field around a model of AgNP aggregates in water, ethanol and chloroform (Figure 3.8). Effective plasmonic coupling was observed at the interface of AgNPs aggregate in chloroform, especially at the nanogaps formed between spherical and triangular AgNPs as well as the edges/tips of the triangular AgNPs. When modeling plasmonic field in ethanol, plasmon-plasmon coupling was also observed but to a significantly lower degree. However, in water, there is no significant plasmonic coupling and only a negligible field enhancement at the edges of AgNPs.

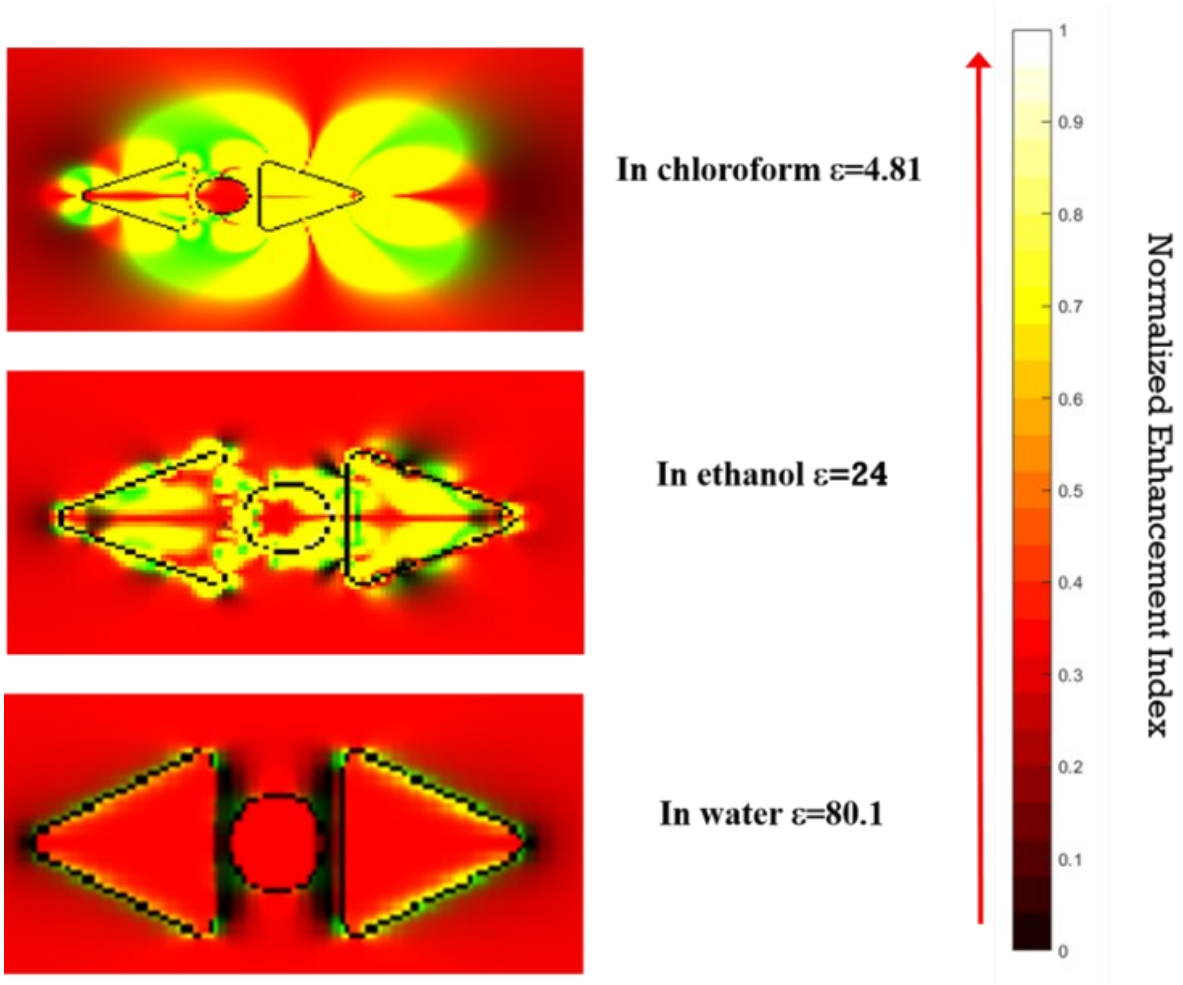

Figure 3.8 Simulated plasmonic field enhancement at the interface of modeled AgNPs aggregate in different solvents.

Based on the simulations of the enhanced plasmonic field in three different solvents, the SERS detection in chloroform could allow the adsorbed pATP to experience the strongest plasmonic field, thus generating intensive SERS signals. Because of this, the SERS signal from pATP at very low concentrations could be detected in chloroform as compared to in water.

3.4 Conclusion and Future Work

Herein, SERS detection was successfully and completely operated in organic solvents by taking advantage of a facile phase transfer of ethanol modified AgNPs from the aqueous phase. In addition, unexpected ultra-high sensitivity of the SERS detector was achieved in some organic solvents, reaching zM or aM levels in methylene chloride and chloroform, respectively. Compared to aqueous solutions, SERS analysis in organic solvents was strongly affected by the coupling of generated electric fields at the AgNP and solvent interface, thus dramatically affecting the electromagnetic enhancement of SERS signals. This solvent effect is associated with the dielectric constant of the solvent.

However, the results obtained above are preliminary. Further validation of the data is needed. In addition, the correlation between sample concentrations and the SERS signal intensities in different organic solvents will be further studied.

The other factors are also necessary to explore in order to fully understand the mechanism determining SERS detection in organic solvents. One of the possible factors could be dissolved oxygen present in the organic solvent, which has been considered the biggest barrier of ultrasensitive SERS detection in aqueous solutions (Nganou et al., 2020). In this computational simulation, the oxygen effect was not taken into account, which suggests that even with dissolved oxygen present, a strong electromagnetic field was still generated in organic solvents with lower dielectric constants. However, compared to aqueous solutions, the concentration of oxygen dissolved in organic solvent might be typically less, and the effect of oxygen in different solvents requires further study. We believe comparing the oxygen effect with the solvent effect could offer a better and deeper understanding of

SERS mechanisms. Furthermore, dissolved oxygen effects may explain the discrepancy between chloroform and methylene chloride and their individual dielectric constants. With very similar dielectric constants, the dissolved oxygen effect may become more significant. Finally, it should be noted that when the LOD is at the aM or zM level, the possibility of the analyte simultaneously being located in the nanogap and the field of the detector is extremely low, which may suggest the propagation of the SERS signal in the media (Nganou et al., 2020). Therefore, the ultra-sensitivity of SERS detection in organic solvent may be considered as a two-step processes involving, first, the SERS signal generation at the AgNPs surface, followed by propagation of the signals within the sample volume.

Chapter 4
Conclusion

This thesis focused on the emerging field of using SERS for environmental analysis by first providing a comprehensive review of SERS metal sensors and second by investigating the effect of solvent on SERS detection sensitivity. SERS is an ultra-sensitive analytical technique, and its portable and affordable nature allows for potential application for on-site environmental analysis. SERS principles have been well studied by both experimental research and theoretical approaches. As a result, researchers have utilized the advantages of the high sensitivity of SERS for chemical sensing, especially for analyte at low concentrations. Even though SERS as an analytical tool has been developed for many different metal sensors, there was no comprehensive review to help the scientific community to overview the field. The review in this thesis summarizes the literature within a framework that emphasizes the scientific principles and different approaches and opportunities for SERS sensor development.

With the systematic review of the mechanisms of reporter signals generated by the interaction between the target metal ions and the SERS sensor, a summary is provided of the sensing methods that are used for detection metal ions. It was found that compared to other types of metal sensor, SERS metal sensor show relatively low LOD and capability of detecting target metal ions at low concentrations. In addition, depending on the sensing methods, enhanced substrate and sample preparation methods can help to improve the sensitivity of the SERS metal sensors. However, because the instability of SERS substrates can greatly affect the SERS signal of the reporter, quantitation using the intensity change of

the reporter molecule result ion inaccuracy and this is a future research challenge. Furthermore, it was recognized that some fundamental understanding of the SERS metal sensors is still missing, including the substrate aggregation control and multiple metal ion detection by using the same reporter molecule. These factors limit the ability of current SERS metal sensors to be simpler and more accurate. The gaps between laboratory research and the real sample detection were identified. In particular, an understanding of the matrix effect on SERS metal sensors is still lacking and needs to be further explored.

In terms of the solvent effect on SERS, both experimental evidence and computational modeling showed that dielectric constant can dramatically affect the SERS detection sensitivity. When the analyte is in the organic solvents with lower dielectric constant, the SERS sensitivity is higher. Additionally, a reliable protocol was developed for SERS detection in organic solvents. However, when in two organic solvents with small difference in the dielectric constant are used other parameters may play a role in determining the sensitivity of the SERS detection, which is currently unclear. For example, as shown in Chapter 3, methylene chloride has a higher dielectric constant but results in higher SERS sensitivity comparing to chloroform. Furthermore, the ultra-sensitive detection (such as zM detection), may suggest SERS field propagation within the sample. Therefore, for future work, in addition to dielectric constant, other parameters of the organic solvent, such as dissolved oxygen, that may affect the SERS sensitivity are needed to be studied to be able to fully understand the solvent effect on SERS. This will result in an enhanced fundamental understanding of the SERS detection and potential for improved SERS detectors. Also, the propagation of the SERS field in organic solvent is of great interest since it could be used for

indirect sensing of the analytes, which could dramatically benefit the on-site environmental analysis.

With the deepening understanding of the mechanisms involved in SERS detection, it will be possible to develop new more sensitive and selective sensors. The comprehensive review of the literature identified many opportunities for research and application of this approach. Experiments on the effects of solvents contribute to this understanding and will lead to additional refinement of SERS. This broadens the potential for SERS sensors that have ultra-high sensitivity and accuracy to be applied widely to environmental analysis.

Bibliography

Alpendurada, M. de F. (2000). Solid-phase microextraction: a promising technique for sample preparation in environmental analysis. *Journal of Chromatography A*, *889*(1–2), 3–14. https://doi.org/10.1016/S0021-9673(00)00453-2

Annavaram, V., Kutsanedzie Y.H., F., Agyekum A., A., Shah, S. A., Zareef, M., Hassan, M. M., … Chen, Q. (2019). NaYF4@Yb,Ho,Au/GO-nanohybrid materials for SERS applications—Pb(II) detection and prediction. *Colloids and Surfaces B: Biointerfaces*, *174*, 598–606. https://doi.org/10.1016/j.colsurfb.2018.11.039

Arjomandi, M., & Shirkhanloo, H. (2019). A review: Analytical methods for heavy metals determination in environment and human samples. *Analytical Methods in Environmental Chemistry Journal*, *2*(03), 97–126. https://doi.org/10.24200/amecj.v2.i03.73

Awual, M. R., Yaita, T., Taguchi, T., Shiwaku, H., Suzuki, S., & Okamoto, Y. (2014). Selective cesium removal from radioactive liquid waste by crown ether immobilized new class conjugate adsorbent. *Journal of Hazardous Materials*, *278*, 227–235. https://doi.org/10.1016/j.jhazmat.2014.06.011

Boyack R, & Ru E. (2009). Investigation of particle shape and size effects in SERS using T-matrix calculations. *Physical Chemistry Chemical Physics*, *11*(34), 7398–7405. https://doi.org/10.1039/B905645A

Breuer, P. L., & Jeffrey, M. I. (2000). Thiosulfate leaching kinetics of gold in the presence of copper and ammonia. *Minerals Engineering*, *13*(10), 1071–1081. https://doi.org/10.1016/S0892-6875(00)00091-1

Canário, C., Ngobeni, P., Katskov, D. A., & Thomassen, Y. (2004). Transverse heated filter atomizer: Atomic absorption spectrometric determination of Pb and Cd in whole blood. *Journal of Analytical Atomic Spectrometry*, *19*(11), 1468–1473. https://doi.org/10.1039/b409022e

Chen, J. L., Yang, P. C., Wu, T., & Lin, Y. W. (2018). Determination of mercury (II) ions based on silver-nanoparticles-assisted growth of gold nanostructures: UV–Vis and surface

enhanced Raman scattering approaches. *Spectrochimica Acta - Part A: Molecular and Biomolecular Spectroscopy*, *199*, 301–307. https://doi.org/10.1016/j.saa.2018.03.077

Chen, Lei, Zhao, Y., Wang, Y., Zhang, Y., Liu, Y., Han, X. X., … Yang, J. (2016). Mercury species induced frequency-shift of molecular orientational transformation based on SERS. *Analyst*, *141*(15), 4782–4788. https://doi.org/10.1039/c6an00945j

Chen, L., Qi, N., Wang, X., Chan, L., You, H., & Li, J. (2014). Ultrasensitive surface-enhanced Raman scattering nanosensor for mercury ion detection based on functionalized silver nanoparticles. *RSC Advances*, *4*(29), 15055–15060. https://doi.org/10.1039/c3ra47492e

Cheng, F., Xu, H., Wang, C., Gong, Z., Tang, C., & Fan, M. (2015). Surface enhanced Raman scattering fiber optic sensor as an ion selective optrode: The example of Cd2+ detection. *RSC Advances*, *4*(110), 64683–64687. https://doi.org/10.1039/c4ra11260a

Cheng, Y., Li, J., Deng, S., & Sun, F. (2019). AgNPs@Ag(I)-AMTD metal-organic gel-nanocomposites act as a SERS probe for the detection of Hg2+. *Composites Communications*, *13*, 75–79. https://doi.org/10.1016/j.coco.2019.03.005

Chung, E., Gao, R., Ko, J., Choi, N., Lim, D. W., Lee, E. K., … Choo, J. (2013). Trace analysis of mercury(ii) ions using aptamer-modified Au/Ag core-shell nanoparticles and SERS spectroscopy in a microdroplet channel. *Lab on a Chip*, *13*(2), 260–266. https://doi.org/10.1039/c2lc41079f

Cialla, D., März, A., Böhme, R., Theil, F., Weber, K., Schmitt, M., & Popp, J. (2012). Surface-enhanced Raman spectroscopy (SERS): Progress and trends. *Analytical and Bioanalytical Chemistry*, *403*, 27–54. https://doi.org/10.1007/s00216-011-5631-x

Dasary, S. S. R., Jones, Y. K., Barnes, S. L., Ray, P. C., & Singh, A. K. (2016). Alizarin dye based ultrasensitive plasmonic SERS probe for trace level cadmium detection in drinking water. *Sensors and Actuators, B: Chemical*, *224*, 65–72. https://doi.org/10.1016/j.snb.2015.10.003

Dasary, S. S. R., Singh, A. K., Senapati, D., Yu, H., & Ray, P. C. (2009). Gold nanoparticle based label-free SERS probe for ultrasensitive and selective detection of trinitrotoluene. *Journal of the American Chemical Society*, *131*(38), 13806–13812. https://doi.org/10.1021/ja905134d

Ding, X., Kong, L., Wang, J., Fang, F., Li, D., & Liu, J. (2013). Highly sensitive SERS detection of Hg2+ ions in aqueous media using gold nanoparticles/graphene heterojunctions. *ACS Applied Materials and Interfaces*, *5*(15), 7072–7078. https://doi.org/10.1021/am401373e

Ding, Y., Wang, S., Li, J., & Chen, L. (2016). Nanomaterial-based optical sensors for mercury ions. *TrAC - Trends in Analytical Chemistry*, *82*, 175–190. https://doi.org/10.1016/j.trac.2016.05.015

Docherty, J., Mabbott, S., Smith, E., Faulds, K., Davidson, C., Reglinski, J., & Graham, D. (2016). Detection of potentially toxic metals by SERS using salen complexes. *Analyst*, *141*(20), 5857–5863. https://doi.org/10.1039/c6an01584k

Docherty, J., Mabbott, S., Smith, W. E., Reglinski, J., Faulds, K., Davidson, C., & Graham, D. (2015). Determination of metal ion concentrations by SERS using 2,2′-bipyridyl complexes. *Analyst*, *140*(19), 6538–6543. https://doi.org/10.1039/c5an01525a

Doering, W. E., & Nie, S. (2002). Single-molecule and single-nanoparticle SERS: Examining the roles of surface active sites and chemical enhancement. *Journal of Physical Chemistry B*, *106*(2), 311–317. https://doi.org/10.1021/jp011730b

Du, Y., Liu, R., Liu, B., Wang, S., Han, M. Y., & Zhang, Z. (2013). Surface-enhanced raman scattering chip for femtomolar detection of mercuric ion (II) by ligand exchange. *Analytical Chemistry*, *85*(6), 3160–3165. https://doi.org/10.1021/ac303358w

Duan, J., Yang, M., Lai, Y., Yuan, J., & Zhan, J. (2012). A colorimetric and surface-enhanced Raman scattering dual-signal sensor for Hg 2+ based on Bismuthiol II-capped gold nanoparticles. *Analytica Chimica Acta*, *723*, 88–93. https://doi.org/10.1016/j.aca.2012.02.031

Duan, Z., Zhang, X., Ye, T., Zhang, X., Dong, S., Liu, J., … Jiang, C. (2018). Ultrasensitive Au nanooctahedron micropinball sensor for mercury ions. *ACS Applied Materials & Interfaces*, *10*(30), 25737–25743. https://doi.org/10.1021/ACSAMI.8B04414

Dugandžić, V., Kupfer, S., Jahn, M., Henkel, T., Weber, K., Cialla-May, D., & Popp, J. (2019). A SERS-based molecular sensor for selective detection and quantification of copper(II) ions. *Sensors and Actuators, B: Chemical*, *279*, 230–237. https://doi.org/10.1016/j.snb.2018.09.098

Duruibe, J. O., Ogwuegbu, M. O. C., & Egwurugwu. (2007). Heavy metal pollution and human biotoxic effects. *International Journal of Physical Sciences*, *2*(5), 112–118. https://doi.org/10.5897/IJPS.9000289

El-Said, W. A., Cho, H. Y., & Choi, J. W. (2017). SERS Application for Analysis of Live Single Cell. *NANOPLASMONICS*, 361.

Fitzpatrick, L. J., & Dean, J. R. (2002). Extraction solvent selection in environmental analysis. *Analytical Chemistry*, *74*(1), 74–79. https://doi.org/10.1021/ac001336u

Fleischmann, M., Hendra, P. J., & McQuillan, A. J. (1974). Raman spectra of pyridine adsorbed at a silver electrode. *Chemical Physics Letters*, *26*(2), 163–166. https://doi.org/10.1016/0009-2614(74)85388-1

Fornasaro S, Alsamad F, Baia M, Batista L, Beleites C, Byrne H, … Bonifacio A. (2020). Surface enhanced Raman spectroscopy for quantitative analysis: results of a large-scale european multi-instrument interlaboratory study. *Analytical Chemistry*, *92*(5), 4053–4064. https://doi.org/10.1021/acs.analchem.9b05658

Franciscato, D. S., Matias, T. A., Shinohara, J., Gonçalves, J. M., Coelho, N. P., Fernandes, C. S., … de Souza, V. R. (2018). Thiosemicarbazone@Gold nanoparticle hybrid as selective SERS substrate for Hg2+ ions. *Spectrochimica Acta - Part A: Molecular and Biomolecular Spectroscopy*, *204*, 174–179. https://doi.org/10.1016/j.saa.2018.06.038

Frost, M. S., Dempsey, M. J., & Whitehead, D. E. (2015). Highly sensitive SERS detection of Pb2+ ions in aqueous media using citrate functionalised gold nanoparticles. *Sensors and Actuators, B: Chemical*, *221*, 1003–1008. https://doi.org/10.1016/j.snb.2015.07.001

Fu, C., Xu, W., Wang, H., Ding, H., Liang, L., Cong, M., & Xu, S. (2014). DNAzyme-based plasmonic nanomachine for ultrasensitive selective surface-enhanced raman scattering detection of lead ions via a particle-on-a-film hot spot construction. *Analytical Chemistry*, *86*(23), 11494–11497. https://doi.org/10.1021/ac5038736

Fu, S., Guo, X., Wang, H., Yang, T., Wen, Y., & Yang, H. (2014). Detection of trace mercury ions in water by a novel Raman probe. *Sensors and Actuators, B: Chemical*, *199*, 108–114. https://doi.org/10.1016/j.snb.2014.03.091

García, F., & Howie, A. (1998). Relativistic electron energy loss and electron-induced photon emission in inhomogeneous dielectrics. *Physical Review Letters*, *80*(23), 5180–5183. https://doi.org/10.1103/PhysRevLett.80.5180

García, F., & Howie, A. (2002). Retarded field calculation of electron energy loss in inhomogeneous dielectrics. *Physical Review B - Condensed Matter and Materials Physics*, *65*(11), 1154181–11541817. https://doi.org/10.1103/PhysRevB.65.115418

Ghosh, S. K., Nath, S., Kundu, S., Esumi, K., & Pal, T. (2004). Solvent and ligand effects on the localized surface plasmon resonance (LSPR) of gold colloids. *The Journal of Physical Chemistry B*, *108*(37), 13963–13971. https://doi.org/10.1021/jp047021q

Gong, L., Zhao, Z., Lv, Y. F., Huan, S. Y., Fu, T., Zhang, X. B., … Yu, R. Q. (2015). DNAzyme-based biosensors and nanodevices. *Chemical Communications*, *51*(6), 979–995. https://doi.org/10.1039/c4cc06855f

Gu, X., Trujillo, M. J., Olson, J. E., & Camden, J. P. (2018). SERS sensors: recent developments and a generalized classification scheme based on the signal origin. *Annual Review of Analytical Chemistry*, *11*, 147–169. https://doi.org/10.1146/annurev-anchem-061417-125724

Guerrini, L., & Alvarez-Puebla, R. A. (2021). Surface-enhanced Raman scattering sensing of transition metal ions in waters. *ACS Omega*, *6*, 1054–1063. American Chemical Society. https://doi.org/10.1021/acsomega.0c05261

Guerrini, L., Rodriguez-Loureiro, I., Correa-Duarte, M. A., Lee, Y. H., Ling, X. Y., García De Abajo, F. J., & Alvarez-Puebla, R. A. (2014). Chemical speciation of heavy metals by surface-enhanced Raman scattering spectroscopy: Identification and quantification of inorganic- and methyl-mercury in water. *Nanoscale*, *6*(14), 8368–8375. https://doi.org/10.1039/c4nr01464b

Guo, X., Chen, F., Wang, F., Wu, Y., Ying, Y., Wen, Y., … Ke, Q. (2020). Recyclable Raman chip for detection of trace Mercury ions. *Chemical Engineering Journal*, *390*, 124528. https://doi.org/10.1016/j.cej.2020.124528

Guo, Yanyan, Li, D., Zheng, S., Xu, N., & Deng, W. (2020). Utilizing Ag–Au core-satellite structures for colorimetric and surface-enhanced Raman scattering dual-sensing of Cu (II). *Biosensors and Bioelectronics*, *159*, 112192. https://doi.org/10.1016/j.bios.2020.112192

Guo, Yue, Tao, Y., Ma, X., Jin, J., Wen, S., Ji, W., … Ozaki, Y. (2018). A dual colorimetric and SERS detection of Hg2+ based on the stimulus of intrinsic oxidase-like catalytic activity of Ag-CoFe2O4/reduced graphene oxide nanocomposites. *Chemical Engineering Journal*, *350*, 120–130. https://doi.org/10.1016/j.cej.2018.05.135

Guselnikova, O., Postnikov, P., Erzina, M., Kalachyova, Y., Švorčík, V., & Lyutakov, O. (2017). Pretreatment-free selective and reproducible SERS-based detection of heavy metal ions on DTPA functionalized plasmonic platform. *Sensors and Actuators, B: Chemical*, *253*, 830–838. https://doi.org/10.1016/j.snb.2017.07.018

Halvorson, R. A., & Vikesland, P. J. (2010). Surface-enhanced Raman spectroscopy (SERS) for environmental analyses. *Environmental Science and Technology*, *44*(20), 7749–7755. https://doi.org/10.1021/ES101228Z

Han, D., Lim, S. Y., Kim, B. J., Piao, L., & Chung, T. D. (2010). Mercury(ii) detection by SERS based on a single gold microshell. *Chemical Communications*, *46*(30), 5587–5589. https://doi.org/10.1039/c0cc00895h

Hao, B., Bu, X., Wu, J., Ding, Y., Zhang, L., Zhao, B., & Tian, Y. (2020). Determination of Hg2+ in water based on acriflavine functionalized AgNPs by SERS. *Microchemical Journal*, *155*, 104736. https://doi.org/10.1016/j.microc.2020.104736

Hao, J., Han, M. J., Han, S., Meng, X., Su, T. L., & Wang, Q. K. (2015). SERS detection of arsenic in water: A review. *Journal of Environmental Sciences*, *36*, 152–162. https://doi.org/10.1016/j.jes.2015.05.013

He, Q., Han, Y., Huang, Y., Gao, J., Gao, Y., Han, L., & Zhang, Y. (2021). Reusable dual-enhancement SERS sensor based on graphene and hybrid nanostructures for ultrasensitive lead (II) detection. *Sensors and Actuators B: Chemical*, *341*, 130031. https://doi.org/10.1016/J.SNB.2021.130031

Ho, W. K. H., Bao, Z. Y., Gan, X., Wong, K. Y., Dai, J., & Lei, D. (2019). Probing conformation change and binding mode of metal ion-carboxyl coordination complex through Resonant Surface-Enhanced Raman Spectroscopy and Density Functional Theory. *Journal of Physical Chemistry Letters*, *10*(16), 4692–4698. https://doi.org/10.1021/acs.jpclett.9b01435

Hohenester, U., & Krenn, J. (2005). Surface plasmon resonances of single and coupled metallic nanoparticles: A boundary integral method approach. *Physical Review B - Condensed Matter and Materials Physics*, *72*(19), 195429. https://doi.org/10.1103/PhysRevB.72.195429

Ibusuki, T., & Saito, Y. (1976). Coordinate bonding properties of complexes of pyridine with platinum(II) and mercury(II) chlorides. *Inorganica Chimica Acta*, *19*(C), 87–90. https://doi.org/10.1016/S0020-1693(00)91078-8

Ji, W., Li, L., Zhang, Y., Wang, X., & Ozaki, Y. (2021). Recent advances in surface-enhanced Raman scattering-based sensors for the detection of inorganic ions: sensing

mechanism and beyond. *Journal of Raman Spectroscopy*, *52*, 468–481. https://doi.org/10.1002/jrs.5975

Kandjani, A. E., Sabri, Y. M., Mohammad-Taheri, M., Bansal, V., & Bhargava, S. K. (2015). Detect, remove and reuse: A new paradigm in sensing and removal of Hg (II) from wastewater via SERS-active ZnO/Ag nanoarrays. *Environmental Science and Technology*, *49*(3), 1578–1584. https://doi.org/10.1021/es503527e

Kang, Y., Zhang, H., Zhang, L., Wu, T., Sun, L., Jiang, D., & Du, Y. (2017). In situ preparation of Ag nanoparticles by laser photoreduction as SERS substrate for determination of Hg2+. *Journal of Raman Spectroscopy*, *48*(3), 399–404. https://doi.org/10.1002/jrs.5044

Kedia, A., & Senthil Kumar, P. (2012). Precursor-driven nucleation and growth kinetics of gold nanostars. *Journal of Physical Chemistry C*, *116*(2), 1679–1686. https://doi.org/10.1021/jp2063518

Kelly, K. L., Coronado, E., Zhao, L. L., & Schatz, G. C. (2003). The optical properties of metal nanoparticles: The influence of size, shape, and dielectric environment. *Journal of Physical Chemistry B*, *107*(3), 668–677. https://doi.org/10.1021/jp026731y

Kim, K., Lee, J. W., & Shin, S. (2013). Cyanide SERS as a platform for detection of volatile organic compounds and hazardous transition metal ions. *Analyst*, *138*(10), 2988–2994. https://doi.org/10.1039/c3an00105a

Kneipp, J., Kneipp, H., & Kneipp, K. (2008). SERS—a single-molecule and nanoscale tool for bioanalytics. *Chemical Society Reviews*, *37*(5), 1052–1060. https://doi.org/10.1039/b708459p

Kulkarni, A. P., Munechika, K., Noone, K. M., Smith, J. M., & Ginger, D. S. (2009). Phase transfer of large anisotropic plasmon resonant silver nanoparticles from aqueous to organic solution. *Langmuir*, *25*(14), 7932–7939. https://doi.org/10.1021/la900600z

Kwan Kim, Won Lee, J., & Soo Shin, K. (2013). Cyanide SERS as a platform for detection of volatile organic compounds and hazardous transition metal ions. *Analyst*, *138*(10), 2988–2994. https://doi.org/10.1039/C3AN00105A

Lagos, M. J., Trügler, A., Hohenester, U., & Batson, P. E. (2017). Mapping vibrational surface and bulk modes in a single nanocube. *Nature*, *543*(7646), 529–532. https://doi.org/10.1038/nature21699

Laurence, T. A., Braun, G., Talley, C., Schwartzberg, A., Moskovits, M., Reich, N., & Huser, T. (2009). Rapid, solution-based characterization of optimized SERS nanoparticle substrates. *Journal of the American Chemical Society*, *131*(1), 162–169. https://doi.org/10.1021/ja806236k

Lee, Y. F., & Huang, C. C. (2011). Colorimetric assay of lead ions in biological samples using a nanogold-based membrane. *ACS Applied Materials and Interfaces*, *3*(7), 2747–2754. https://doi.org/10.1021/am200535s

Leung, K. M., & Liu, Y. F. (1990). Full vector wave calculation of photonic band structures in face-centered-cubic dielectric media. *Physical Review Letters*, *65*(21), 2646. https://doi.org/10.1103/PhysRevLett.65.2646

Li, C., Fan, P., Liang, A., Liu, Q., & Jiang, Z. (2018). Aptamer based determination of Pb(II) by SERS and by exploiting the reduction of HAuCl4 by H2O2 as catalyzed by graphene oxide nanoribbons. *Microchimica Acta*, *185*(3), 1–8. https://doi.org/10.1007/s00604-018-2714-9

Li, C., Wang, H., Luo, Y., Wen, G., & Jiang, Z. (2019). A novel gold nanosol SERS quantitative analysis method for trace Na + based on carbon dot catalysis. *Food Chemistry*, *289*, 531–536. https://doi.org/10.1016/j.foodchem.2019.03.032

Li, C., Yao, D., Jiang, X., Liang, A., & Jiang, Z. (2020). Strong catalysis of silver-doped carbon nitride nanoparticles and their application to aptamer SERS and RRS coupled dual-mode detection of ultra-trace K+. *Journal of Materials Chemistry C*, *8*(32), 11088–11101. https://doi.org/10.1039/d0tc01581d

Li, D., Ma, Y., Duan, H., Jiang, F., Deng, W., & Ren, X. (2018). Fluorescent/SERS dual-sensing and imaging of intracellular Zn2+. *Analytica Chimica Acta*, *1038*, 148–156. https://doi.org/10.1016/j.aca.2018.07.020

Li, F., Wang, J., Lai, Y., Wu, C., Sun, S., He, Y., & Ma, H. (2013). Ultrasensitive and selective detection of copper (II) and mercury (II) ions by dye-coded silver nanoparticle-based SERS probes. *Biosensors and Bioelectronics*, *39*(1), 82–87. https://doi.org/10.1016/j.bios.2012.06.050

Li, H., Chen, Q., Hassan, M. M., Ouyang, Q., Jiao, T., Xu, Y., & Chen, M. (2018). AuNS@Ag core-shell nanocubes grafted with rhodamine for concurrent metal-enhanced fluorescence and surfaced enhanced Raman determination of mercury ions. *Analytica Chimica Acta*, *1018*, 94–103. https://doi.org/10.1016/j.aca.2018.01.050

Li, J., Zheng, B., Zheng, Z., Li, Y., & Wang, J. (2020). Highly sensitive and selective colorimetric and SERS dual-mode detection of arsenic (III) based on glutathione functionalized gold nanoparticles. *Sensors and Actuators Reports*, *2*(1), 100013. https://doi.org/10.1016/j.snr.2020.100013

Li, Z., Ma, Z. der K. T. J., Yuan, Z., & Huang, L. (2014). A review of soil heavy metal pollution from mines in China: Pollution and health risk assessment. *Science of the Total Environment*, *468–469*, 843–853. https://doi.org/10.1016/j.scitotenv.2013.08.090

Liu Z, Yang Z, Cui l, Ren B, and, & Tian z. (2007). Electrochemically roughened palladium electrodes for surface-enhanced Raman spectroscopy: methodology, mechanism, and application. *Journal of Physical Chemistry C*, *111*(4), 1770–1775. https://doi.org/10.1021/JP066122G

Liu, H., Guo, Y., Wang, Y., Zhang, H., Ma, X., Wen, S., … Ozaki, Y. (2021). A nanozyme-based enhanced system for total removal of organic mercury and SERS sensing. *Journal of Hazardous Materials*, *405*, 124642. https://doi.org/10.1016/j.jhazmat.2020.124642

Liu, J., & Lu, Y. (2004). Accelerated color change of gold nanoparticles assembled by DNAzymes for simple and fast colorimetric Pb2+ detection. *Journal of the American Chemical Society*, *126*(39), 12298–12305. https://doi.org/10.1021/ja046628h

Liu, R., Liu, X., Tang, Y., Wu, L., Hou, X., & Lv, Y. (2011). Highly sensitive immunoassay based on immunogold-silver amplification and inductively coupled plasma mass spectrometric detection. *Analytical Chemistry*, *83*(6), 2330–2336. https://doi.org/10.1021/ac103265z

Liu, X., Liu, M., Lu, Y., Wu, C., Xu, Y., Lin, D., … Feng, S. (2018). Facile Ag-film based surface enhanced Raman spectroscopy using DNA molecular switch for ultra-sensitive mercury ions detection. *Nanomaterials, 8*, 596. https://doi.org/10.3390/NANO8080596

Liu, Y., Wu, Y., Guo, X., Wen, Y., & Yang, H. (2019). Rapid and selective detection of trace Cu2+ by accumulation- reaction-based Raman spectroscopy. *Sensors and Actuators, B: Chemical*, *283*, 278–283. https://doi.org/10.1016/j.snb.2018.12.043

Lou, T., Chen, L., Chen, Z., Wang, Y., Chen, L., & Li, J. (2011). Colorimetric detection of trace copper ions based on catalytic leaching of silver-coated gold nanoparticles. *ACS Applied Materials and Interfaces*, *3*(11), 4215–4220. https://doi.org/10.1021/am2008486

Lu, C., Huang, Z., Liu, B., Liu, Y., Ying, Y., & Liu, J. (2017). Poly-cytosine DNA as a High-Affinity Ligand for Inorganic Nanomaterials. *Angewandte Chemie - International Edition*, *56*(22), 6208–6212. https://doi.org/10.1002/anie.201702998

Lu, Y., Zhong, J., Yao, G., & Huang, Q. (2018). A label-free SERS approach to quantitative and selective detection of mercury (II) based on DNA aptamer-modified SiO2@Au core/shell nanoparticles. *Sensors and Actuators B: Chemical*, *258*, 365–372. https://doi.org/10.1016/J.SNB.2017.11.110

Lyon, L. A., Keating, C. D., Fox, A. P., Baker, B. E., He, L., Nicewarner, S. R., … Natan, M. J. (1998). Raman spectroscopy. *Analytical Chemistry*, *70*, 341–361.

Ma, J., Feng, G., Ying, Y., Shao, Y., She, Y., Zheng, L., … Wang, J. (2021). Sensitive SERS assay for glyphosate based on the prevention of l-cysteine inhibition of a Au-Pt nanozyme. *Analyst*, *146*(3), 956–963. https://doi.org/10.1039/d0an01919d

Ma, P., Liang, F., Diao, Q., Wang, D., Yang, Q., Gao, D., … Wang, X. (2015). Selective and sensitive SERS sensor for detection of Hg2+ in environmental water base on rhodamine-bonded and amino group functionalized SiO2-coated Au-Ag core-shell nanorods. *RSC Advances*, *5*(41), 32168–32174. https://doi.org/10.1039/c5ra04423e

Ma, W., Sun, M., Xu, L., Wang, L., Kuang, H., & Xu, C. (2013). A SERS active gold nanostar dimer for mercury ion detection. *Chemical Communications*, *49*(44), 4989–4991. https://doi.org/10.1039/c3cc39087j

Makam, P., Shilpa, R., Kandjani, A. E., Periasamy, S. R., Sabri, Y. M., Madhu, C., … Govindaraju, T. (2018). SERS and fluorescence-based ultrasensitive detection of mercury in water. *Biosensors and Bioelectronics*, *100*, 556–564. https://doi.org/10.1016/j.bios.2017.09.051

Marquez, L. A., & Dunford, H. B. (1997). Mechanism of the oxidation of 3,5,3',5'-tetramethylbenzidine by myeloperoxidase determined by transient- and steady-state kinetics. *Biochemistry*, *36*(31), 9349–9355. https://doi.org/10.1021/bi970595j

Miyake, Y., Togashi, H., Tashiro, M., Yamaguchi, H., Oda, S., Kudo, M., … Ono, A. (2006). MercuryII-mediated formation of thymine-HgII-thymine base pairs in DNA duplexes. *Journal of the American Chemical Society*, *128*(7), 2172–2173. https://doi.org/10.1021/ja056354d

Mizutani, G., & Ushioda, S. (1989). Normal mode analysis of surface adsorbed and coordinated pyridine molecule. *The Journal of Chemical Physics*, *91*(1), 598–602. https://doi.org/10.1063/1.457661

Morrison, D., Rothenbroker, M., & Li, Y. (2018). DNAzymes: selected for applications. *Small Methods*, *2*(3), 1700319. https://doi.org/10.1002/smtd.201700319

Mosier-Boss, P. A. (2017). Review of SERS substrates for chemical sensing. *Nanomaterials*, *7*(6), 142. https://doi.org/10.3390/nano7060142

Moskovits, M., Tay, L.-L., Yang, J., & Haslett, T. (2007). SERS and the single molecule. *Optical Properties of Nanostructured Random Media*. 215–227. Springer Berlin Heidelberg. https://doi.org/10.1007/3-540-44948-5_10

Ndokoye, P., Ke, J., Liu, J., Zhao, Q., & Li, X. (2014). L-cysteine-modified gold nanostars for SERS-based copper ions detection in aqueous media. *Langmuir*, *30*(44), 13491–13497. https://doi.org/10.1021/la503553y

Nganou, C., Carrier, A. J., Yang, D., Chen, Y., Yu, N., Richards, D. D., … Zhang, X. (2020). Ultrasensitive and eemote SERS enabled by oxygen-free integrated plasmonic field transmission. *Cell Reports Physical Science*, *1*(9), 100189. https://doi.org/10.1016/j.xcrp.2020.100189

Nie, S., & Emory, S. R. (1997). Probing single molecules and single nanoparticles by surface-enhanced Raman scattering. *Science*, *275*(5303), 1102–1106. https://doi.org/10.1126/SCIENCE.275.5303.1102

Ong, T. T. X., Blanch, E. W., & Jones, O. A. H. (2020). Surface enhanced Raman spectroscopy in environmental analysis, monitoring and assessment. *Science of the Total Environment*, *720*. https://doi.org/10.1016/j.scitotenv.2020.137601

Ono, A., Cao, S., Togashi, H., Tashiro, M., Fujimoto, T., MacHinami, T., … Tanaka, Y. (2008). Specific interactions between silver(i) ions and cytosine-cytosine pairs in DNA duplexes. *Chemical Communications*, *0*(39), 4825–4827. https://doi.org/10.1039/b808686a

Ouyang, H., Ling, S., Liang, A., & Jiang, Z. (2018). A facile aptamer-regulating gold nanoplasmonic SERS detection strategy for trace lead ions. *Sensors and Actuators, B: Chemical*, *258*, 739–744. https://doi.org/10.1016/j.snb.2017.12.009

Pantell, R. H., Puthoff, H. E., & Soncini, G. (1968). Stimulated photon-electron scattering. *IEEE Journal of Quantum Electronics*, *4*(11), 905–907. https://doi.org/10.1109/JQE.1968.1074989

Pérez-Jiménez, A. I., Lyu, D., Lu, Z., Liu, G., & Ren, B. (2020). Surface-enhanced Raman spectroscopy: Benefits, trade-offs and future developments. *Chemical Science*, *11*(18), 4563–4577. https://doi.org/10.1039/d0sc00809e

Pilot, R., Signorini, R., Durante, C., Orian, L., Bhamidipati, M., & Fabris, L. (2019). A review on surface-enhanced Raman scattering. *Biosensors*, *9*, 57. https://doi.org/10.3390/bios9020057

Qi, G., Fu, C., Chen, G., Xu, S., & Xu, W. (2015). Highly sensitive SERS sensor for mercury ions based on the catalytic reaction of mercury ion decorated Ag nanoparticles. *RSC Advances*, *5*(61), 49759–49764. https://doi.org/10.1039/c5ra08009f

Qi, L., Xiao, M., Wang, F., Wang, L., Ji, W., Man, T., … Li, L. (2017). Poly-cytosine-mediated nanotags for SERS detection of Hg2+. *Nanoscale*, *9*(37), 14184–14191. https://doi.org/10.1039/c7nr05165d

Qi, Y., Zhao, J., Weng, G. jun, Li, J. jun, Li, X., Zhu, J., & Zhao, J. wu. (2018). A colorimetric/SERS dual-mode sensing method for the detection of mercury(ii) based on rhodanine-stabilized gold nanobipyramids. *Journal of Materials Chemistry C*, *6*(45), 12283–12293. https://doi.org/10.1039/c8tc03980a

Ren, W., Zhu, C., & Wang, E. (2012). Enhanced sensitivity of a direct SERS technique for Hg2+ detection based on the investigation of the interaction between silver nanoparticles and mercury ions. *Nanoscale*, *4*(19), 5902–5909. https://doi.org/10.1039/c2nr31410j

Rojas, R., & Claro, F. (1993). Theory of surface enhanced Raman scattering in colloids. *The Journal of Chemical Physics*, *98*(2), 998–1006. https://doi.org/10.1063/1.464263

Ru, E, Meyer, M., Blackie, E., & Etchegoin, P. (2008). Advanced aspects of electromagnetic SERS enhancement factors at a hot spot. *Journal of Raman Spectroscopy*, *39*(9), 1127–1134. https://doi.org/10.1002/jrs.1945

Ru, Eric, & Etchegoin, P. (2012). Single-molecule surface-enhanced Raman spectroscopy. *Annual review of Physical Chemistry. 63*, 65–87. https://doi.org/10.1146/annurev-physchem-032511-143757

Ru, Eric., & Etchegoin, P. (2008). *Principles of surface-enhanced Raman spectroscopy: and related plasmonic effects.* Elsevier. https://doi.org/10.1016/B978-0-444-52779-0.X0001-3

Rupérez, A., & Laserna, J. J. (1994). Solvent effects on surface-enhanced Raman activity of adsorbates on colloidal silver. *Applied Spectroscopy*, *48*(2), 219–223. https://doi.org/10.1366/0003702944028425

Sabur, A., Havel, M., & Gogotsi, Y. (2008). SERS intensity optimization by controlling the size and shape of faceted gold nanoparticles. *Journal of Raman Spectroscopy*, *39*(1), 61–67. https://doi.org/10.1002/JRS.1814

Sarfo, D. K., Izake, E. L., O'Mullane, A. P., & Ayoko, G. A. (2018). Molecular recognition and detection of Pb(II) ions in water by aminobenzo-18-crown-6 immobilised onto a nanostructured SERS substrate. *Sensors and Actuators, B: Chemical*, *255*, 1945–1952. https://doi.org/10.1016/j.snb.2017.08.223

Sarfo, D. K., Sivanesan, A., Izake, E. L., & Ayoko, G. A. (2017). Rapid detection of mercury contamination in water by surface enhanced Raman spectroscopy. *RSC Advances*, *7*(35), 21567–21575. https://doi.org/10.1039/c7ra02209c

Schatz, G. C., Young, M. A., & Duyne, R. P. (2006). Electromagnetic Mechanism of SERS. *Surface-Enhanced Raman Scattering*, 19–45. Springer Berlin Heidelberg. https://doi.org/10.1007/3-540-33567-6_2

Senapati, T., Senapati, D., Singh, A. K., Fan, Z., Kanchanapally, R., & Ray, P. C. (2011). Highly selective SERS probe for Hg(II) detection using tryptophan-protected popcorn shaped gold nanoparticles. *Chemical Communications*, *47*(37), 10326–10328. https://doi.org/10.1039/c1cc13157e

Sharma, B., Frontiera, R. R., Henry, A. I., Ringe, E., & van Duyne, R. P. (2012). SERS: Materials, applications, and the future. *Materials Today*, *15*(1–2), 16–25. https://doi.org/10.1016/S1369-7021(12)70017-2

Shi, X., Gu, W., Zhang, C., Zhao, L., Li, L., Peng, W., & Xian, Y. (2016). Construction of a graphene/Au-nanoparticles/cucurbit[7]uril-based sensor for Pb2+ sensing. *Chemistry - A European Journal*, *22*(16), 5643–5648. https://doi.org/10.1002/chem.201505034

Shi, Y., Chen, N., Su, Y., Wang, H., & He, Y. (2018). Silicon nanohybrid-based SERS chips armed with an internal standard for broad-range, sensitive and reproducible simultaneous quantification of lead(II) and mercury(II) in real systems. *Nanoscale*, *10*(8), 4010–4018. https://doi.org/10.1039/c7nr07935d

Shi, Y., Wang, H., Jiang, X., Sun, B., Song, B., Su, Y., & He, Y. (2016). Ultrasensitive, specific, recyclable, and reproducible detection of lead ions in real systems through a polyadenine-sssisted, surface-enhanced Raman scattering silicon chip. *Analytical Chemistry*, *88*(7), 3723–3729. https://doi.org/10.1021/acs.analchem.5b04551

Smith, E., & Dent, G. (2019). *Modern Raman spectroscopy: a practical approach*. John Wiley & Sons. https://doi.org/10.1002/9781119440598

Song, C., Li, J., Sun, Y., Jiang, X., Zhang, J., Dong, C., & Wang, L. (2020). Colorimetric/SERS dual-mode detection of mercury ion via SERS-Active peroxidase-like Au@AgPt NPs. *Sensors and Actuators, B: Chemical*, *310*, 127849. https://doi.org/10.1016/j.snb.2020.127849

Song, C., Yang, B., Yang, Y., & Wang, L. (2016). SERS-based mercury ion detections: principles, strategies and recent advances. *Science China Chemistry*, *59*(1), 16–29. https://doi.org/10.1007/s11426-015-5504-9

Song, C., Yang, B., Zhu, Y., Yang, Y., & Wang, L. (2017). Ultrasensitive sliver nanorods array SERS sensor for mercury ions. *Biosensors and Bioelectronics*, *87*, 59–65. https://doi.org/10.1016/j.bios.2016.07.097

Song, L., Mao, K., Zhou, X., & Hu, J. (2016). A novel biosensor based on Au@Ag core-shell nanoparticles for SERS detection of arsenic (III). *Talanta*, *146*, 285–290. https://doi.org/10.1016/j.talanta.2015.08.052

Stiles, P. L., Dieringer, J. A., Shah, N. C., & van Duyne, R. P. (2008). Surface-enhanced Raman spectroscopy. *Annual Review of Analytical Chemistry*, *1*(1), 601–626. https://doi.org/10.1146/annurev.anchem.1.031207.112814

Strak, P., Kempisty, P., Sakowski, K., & Krukowski, S. (2011). Polarization and polarization induced electric field in nitrides-critical evaluation based on DFT studies. *ArXiv Preprint ArXiv*.

Sun, B., Jiang, X., Wang, H., Song, B., Zhu, Y., Wang, H., … He, Y. (2015). Surface-enhancement Raman scattering sensing strategy for discriminating trace mercuric ion (II) from real water samples in sensitive, specific, recyclable, and reproducible manners. *Analytical Chemistry*, *87*(2), 1250–1256. https://doi.org/10.1021/ac503939d

Sun, F., Galvan, D. D., & Yu, Q. (2017). Multi-functional, thiophenol-based surface chemistry for surface-enhanced Raman spectroscopy. *Chemical Communications*, *53*(33), 4550–4561. https://doi.org/10.1039/c7cc01577a

Sun, Z., Du, J., & Jing, C. (2016). Recent progress in detection of mercury using surface enhanced Raman spectroscopy - A review. *Journal of Environmental Sciences*, *39*, 134–143. https://doi.org/10.1016/j.jes.2015.11.009

Sun, Z., Du, J., Lv, B., & Jing, C. (2016). Satellite Fe3O4@SiO2-Au SERS probe for trace Hg2+ detection. *RSC Advances*, *6*(77), 73040–73044. https://doi.org/10.1039/c6ra15044f

Tan, E., Yin, P., Lang, X., Zhang, H., & Guo, L. (2012). A novel surface-enhanced Raman scattering nanosensor for detecting multiple heavy metal ions based on 2-mercaptoisonicotinic acid functionalized gold nanoparticles. *Spectrochimica Acta - Part A: Molecular and Biomolecular Spectroscopy*, *97*, 1007–1012. https://doi.org/10.1016/j.saa.2012.07.114

Tang, W., Bruce Chase, D., Sparks, D. L., & Rabolt, J. F. (2015). Selective and quantitative detection of trace amounts of mercury(II) Ion (Hg2+) and Copper(II) Ion (Cu2+) using surface-enhanced raman scattering (SERS). *Applied Spectroscopy*, *69*(7), 843–849. https://doi.org/10.1366/14-07815

Tao, G. Q., & Wang, J. (2018). Gold nanorod@nanoparticle seed-SERS nanotags/graphene oxide plasmonic superstructured nanocomposities as an "on-off" SERS aptasensor. *Carbon*, *133*, 209–217. https://doi.org/10.1016/j.carbon.2018.03.037

Tchounwou, P. B., Yedjou, C. G., Patlolla, A. K., & Sutton, D. J. (2012). Heavy metal toxicity and the environment. *Molecular, Clinical and Environmental Toxicology* 133–164. Springer, Basel. https://doi.org/10.1007/978-3-7643-8340-4_6

Temiz, H. T., Boyaci, I. H., Grabchev, I., & Tamer, U. (2013). Surface enhanced Raman spectroscopy as a new spectral technique for quantitative detection of metal ions. *Spectrochimica Acta - Part A: Molecular and Biomolecular Spectroscopy*, *116*, 339–347. https://doi.org/10.1016/j.saa.2013.07.071

Teng, Y., Ren, Z., Zhang, Y., Wang, Z., Pan, Z., Shao, K., & She, Y. (2020). Determination of prostate cancer marker Zn2+ with a highly selective surface-enhanced Raman scattering probe on liquid–liquid self-assembled Au nanoarrays. *Talanta*, *209*, 120569. https://doi.org/10.1016/j.talanta.2019.120569

Tian, Z. Q. (2005). Surface-enhanced Raman spectroscopy: advancements and applications. *Journal of Raman Spectroscopy*, *36*(6–7), 466–470. https://doi.org/10.1002/JRS.1378

Tran, T. T., Regan, B., Ekimov, E. A., Mu, Z., Zhou, Y., Gao, W., … Bradac, C. (2019). Anti-Stokes excitation of solid-state quantum emitters for nanoscale thermometry. *Science Advances*, *5*(5), eaav9180. https://doi.org/10.1126/SCIADV.AAV9180

Tsoutsi, D., Guerrini, L., Hermida-Ramon, J. M., Giannini, V., Liz-Marzán, L. M., Wei, A., & Alvarez-Puebla, R. A. (2013). Simultaneous SERS detection of copper and cobalt at ultratrace levels. *Nanoscale*, *5*(13), 5841–5846. https://doi.org/10.1039/c3nr01518a

Ullah, N., Mansha, M., Khan, I., & Qurashi, A. (2018). Nanomaterial-based optical chemical sensors for the detection of heavy metals in water: Recent advances and challenges. *TrAC Trends in Analytical Chemistry*, *100*, 155–166. https://doi.org/10.1016/j.trac.2018.01.002

Urata, H., Yamaguchi, E., Nakamura, Y., & Wada, S. (2011). Pyrimidine-pyrimidine base pairs stabilized by silver(i) ions. *Chemical Communications*, *47*(3), 941–943. https://doi.org/10.1039/c0cc04091f

Vardhan, K. H., Kumar, P. S., & Panda, R. C. (2019). A review on heavy metal pollution, toxicity and remedial measures: Current trends and future perspectives. *Journal of Molecular Liquids*, *290*, 111197. https://doi.org/10.1016/j.molliq.2019.111197

Vareda, J. P., Valente, A. J. M., & Durães, L. (2019). Assessment of heavy metal pollution from anthropogenic activities and remediation strategies: A review. *Journal of Environmental Management*, *246*, 101–118. https://doi.org/10.1016/j.jenvman.2019.05.126

Wang, Haidong, Huang, X., Wen, G., & Jiang, Z. (2019). A dual-model SERS and RRS analytical platform for Pb(II) based on Ag-doped carbon dot catalytic amplification and aptamer regulation. *Scientific Reports*, *9*(1), 1–10. https://doi.org/10.1038/s41598-019-46426-y

Wang, Haolin, Zhang, Z., Chen, C., Liang, A., & Jiang, Z. (2021). Fullerene carbon dot catalytic amplification-aptamer assay platform for ultratrace As3+ utilizing SERS/RRS/Abs trifunctional Au nanoprobes. *Journal of Hazardous Materials*, *403*, 123633. https://doi.org/10.1016/j.jhazmat.2020.123633

Wang, J., Wu, J., Zhang, Y., Zhou, X., Hu, Z., Liao, X., … Sun, P. (2021). Colorimetric and SERS dual-mode sensing of mercury (II) based on controllable etching of Au@Ag core/shell nanoparticles. *Sensors and Actuators, B: Chemical*, *330*, 129364. https://doi.org/10.1016/j.snb.2020.129364

Wang, Yuling, & Irudayaraj, J. (2011). A SERS DNAzyme biosensor for lead ion detection. *Chemical Communications*, *47*(15), 4394–4396. https://doi.org/10.1039/c0cc04140h

Wang, Yulong, Su, Z., Wang, L., Dong, J., Xue, J., Yu, J., … Liu, F. (2017). SERS assay for copper(II) ions based on dual hot-spot model coupling with MarR protein: new Cu2+-specific biorecognition element. *Analytical Chemistry*, *89*(12), 6392–6398. https://doi.org/10.1021/acs.analchem.6b05106

Wei H, Abtahi S, & Vikesland P. (2015). Plasmonic colorimetric and SERS sensors for environmental analysis. *Environmental Science: Nano*, *2*(2), 120–135. https://doi.org/10.1039/C4EN00211C

Wen, G., Xiao, Y., Chen, S., Zhang, X., & Jiang, Z. (2021). A nanosol SERS/RRS aptamer assay of trace cobalt(ii) by covalent organic framework BtPD-loaded nanogold catalytic amplification. *Nanoscale Advances*, 3846–3859. https://doi.org/10.1039/d1na00208b

Wu, X., Tang, L., Ma, W., Xu, L., Liu, L., Kuang, H., & Xu, C. (2015). SERS-active Au NR oligomer sensor for ultrasensitive detection of mercury ions. *RSC Advances*, *5*(100), 81802–81807. https://doi.org/10.1039/c5ra14593g

Wu, Y., Jiang, T., Wu, Z., & Yu, R. (2018). Internal standard-based SERS aptasensor for ultrasensitive quantitative detection of Ag+ ion. *Talanta*, *185*, 30–36. https://doi.org/10.1016/j.talanta.2018.03.014

Wu, Y., Jiang, T., Wu, Z., & Yu, R. (2018). Novel ratiometric surface-enhanced raman spectroscopy aptasensor for sensitive and reproducible sensing of Hg2+. *Biosensors and Bioelectronics*, *99*, 646–652. https://doi.org/10.1016/j.bios.2017.08.041

Wuana, R. A., Okieimen, F. E., Montuelle, B., & Steinman, A. D. (2011). Heavy metals in contaminated soils: a review of sources, chemistry, risks and best available strategies for remediation. *International Scholarly Research Network ISRN Ecology*, *20*. https://doi.org/10.5402/2011/402647

Xu, L., Yin, H., Ma, W., Kuang, H., Wang, L., & Xu, C. (2015). Ultrasensitive SERS detection of mercury based on the assembled gold nanochains. *Biosensors and Bioelectronics*, *67*, 472–476. https://doi.org/10.1016/j.bios.2014.08.088

Xu, S., Cao, X., & Zhou, Y. (2019). Polyvinylpyrrolidine-functionalized silver nanoparticles for SERS based determination of copper(II). *Microchimica Acta*, *186*(8), 1–6. https://doi.org/10.1007/s00604-019-3664-6

Xu, W., Zhao, A., Zuo, F., Jafar Hussain, H. M., & Khan, R. (2019). A "turn-off" SERS aptasensor based DNAzyme-gold nanorod for ultrasensitive lead ion detection. *Analytica Chimica Acta: X*, *2*, 100020. https://doi.org/10.1016/j.acax.2019.100020

Xu, W., Zhao, A., Zuo, F., Khan, R., Hussain, H. M. J., & Li, J. (2020). A highly sensitive DNAzyme-based SERS biosensor for quantitative detection of lead ions in human serum. *Analytical and Bioanalytical Chemistry*, *412*(19), 4565–4574. https://doi.org/10.1007/s00216-020-02709-2

Xu, Z., Zhang, L., Mei, B., Tu, J., Wang, R., Chen, M., & Cheng, Y. (2018). A rapid surface-enhanced Raman scattering (SERS) method for Pb2+ detection using L-cysteine-modified Ag-coated Au nanoparticles with core-shell nanostructure. *Coatings*, *8*(11), 394. https://doi.org/10.3390/COATINGS8110394

Yan, S., Chu, F., Zhang, H., Yuan, Y., Huang, Y., Liu, A., … Wen, W. (2019). Rapid, one-step preparation of SERS substrate in microfluidic channel for detection of molecules and heavy metal ions. *Spectrochimica Acta - Part A: Molecular and Biomolecular Spectroscopy*, *220*, 117113. https://doi.org/10.1016/j.saa.2019.05.018

Yang, B., Chen, X., Liu, R., Liu, B., & Jiang, C. (2015). Target induced aggregation of modified Au@Ag nanoparticles for surface enhanced Raman scattering and its ultrasensitive detection of arsenic(III) in aqueous solution. *RSC Advances*, *5*(95), 77755–77759. https://doi.org/10.1039/c5ra15954g

Yang, D., Liu, X., Zhou, Y., Luo, L., Zhang, J., Huang, A., … Tang, L. (2017). Aptamer-based biosensors for detection of lead(ii) ion: a review. *Analytical Methods*, *9*(13), 1976–1990. https://doi.org/10.1039/c7ay00477j

Yang, P. C., Lin, P. H., Huang, C. C., Wu, T., & Lin, Y. W. (2020). Determination of Hg(II) based on the inhibited catalytic growth of surface-enhanced Raman scattering-active gold

nanoparticles on a patterned hydrophobic paper substrate. *Microchemical Journal*, *157*, 104983. https://doi.org/10.1016/j.microc.2020.104983

Yang, S., Dai, X., Stogin, B. B., & Wong, T. S. (2016). Ultrasensitive surface-enhanced Raman scattering detection in common fluids. *Proceedings of the National Academy of Sciences of the United States of America*, *113*(2), 268–273. https://doi.org/10.1073/pnas.1518980113

Yang, X., He, Y., Wang, X., & Yuan, R. (2017). A SERS biosensor with magnetic substrate CoFe2O4 @ Ag for sensitive detection of Hg2+. *Applied Surface Science*, *416*, 581–586. https://doi.org/10.1016/j.apsusc.2017.04.106

Ye, L., Wen, G., Ouyang, H., Liu, Q., Liang, A., & Jiang, Z. (2016). A novel and highly sensitive nanocatalytic surface plasmon resonance-scattering analytical platform for detection of trace Pb ions. *Scientific Reports*, *6*(1), 1–10. https://doi.org/10.1038/srep24150

Ye, Y., Liu, H., Yang, L., & Liu, J. (2012). Sensitive and selective SERS probe for trivalent chromium detection using citrate attached gold nanoparticles. *Nanoscale*, *4*(20), 6442–6448. https://doi.org/10.1039/c2nr31985c

Yilmaz, M., Babur, E., Ozdemir, M., Gieseking, R. L., Dede, Y., Tamer, U., … Demirel, G. (2017). Nanostructured organic semiconductor films for molecular detection with surface-enhanced Raman spectroscopy. *Nature Materials*, *16*(9), 918–924. https://doi.org/10.1038/nmat4957

Yin, J., Wu, T., Song, J., Zhang, Q., Liu, S., Xu, R., & Duan, H. (2011). SERS-active nanoparticles for sensitive and selective detection of cadmium ion (Cd2+). *Chemistry of Materials*, *23*(21), 4756–4764. https://doi.org/10.1021/cm201791r

Young, A. T. (1981). Rayleigh scattering. *Applied Optics*, *20*(4), 533–535. https://doi.org/10.1364/AO.20.000533

Zamarion, V. M., Timm, R. A., Araki, K., & Toma, H. E. (2008). Ultrasensitive SERS nanoprobes for hazardous metal ions based on trimercaptotriazine-modified gold nanoparticles. *Inorganic Chemistry*, *47*(8), 2934–2936. https://doi.org/10.1021/ic800122v

Zeng, Y., Ren, J., Shen, A., & Hu, J. (2016). Field and pretreatment-free detection of heavy-metal Ions in organic polluted water through an alkyne-coded SERS test kit. *ACS Applied Materials and Interfaces*, *8*(41), 27772–27778. https://doi.org/10.1021/acsami.6b09722

Zeng, Y., Wang, L., Zeng, L., Shen, A., & Hu, J. (2017). A label-free SERS probe for highly sensitive detection of Hg2+ based on functionalized Au@Ag nanoparticles. *Talanta*, *162*, 374–379. https://doi.org/10.1016/j.talanta.2016.09.062

Zhang, Q., Li, N., Goebl, J., Lu, Z., & Yin, Y. (2011). A systematic study of the synthesis of silver nanoplates: Is citrate a "magic" reagent? *Journal of the American Chemical Society*, *133*(46), 18931–18939. https://doi.org/10.1021/ja2080345

Zhang, X., Dai, Z., Si, S., Zhang, X., Wu, W., Deng, H., … Jiang, C. (2017). Ultrasensitive SERS substrate integrated with uniform subnanometer scale "hot spots" created by a graphene spacer for the detection of mercury ions. *Small*, *13*(9), 1603347. https://doi.org/10.1002/smll.201603347

Zhang, Z., Ma, P., Li, J., Sun, Y., Shi, H., Chen, N., … Chen, H. (2019). Colorimetric and SERS dual-mode detection of lead Ions based on Au-Ag core-shell nanospheres: featuring quick screening with ultra-high sensitivity. *Optics Express*, *27*(20), 29248. https://doi.org/10.1364/oe.27.029248

Zhao, L., Gu, W., Zhang, C., Shi, X., & Xian, Y. (2016). In situ regulation nanoarchitecture of Au nanoparticles/reduced graphene oxide colloid for sensitive and selective SERS detection of lead ions. *Journal of Colloid and Interface Science*, *465*, 279–285. https://doi.org/10.1016/j.jcis.2015.11.073

Zhao, Q., Zhang, H., Fu, H., Wei, Y., & Cai, W. (2020). Raman reporter-assisted Au nanorod arrays SERS nanoprobe for ultrasensitive detection of mercuric ion (Hg2+) with superior

anti-interference performances. *Journal of Hazardous Materials*, *398*, 122890. https://doi.org/10.1016/j.jhazmat.2020.122890

Zheng, P., Li, M., Jurevic, R., Cushing, S. K., Liu, Y., & Wu, N. (2015). A gold nanohole array based surface-enhanced Raman scattering biosensor for detection of silver(i) and mercury(ii) in human saliva. *Nanoscale*, *7*(25), 11005–11012. https://doi.org/10.1039/c5nr02142a

Zheng, P., Shi, X., Curtin, K., Yang, F., & Wu, N. (2017). Detection of mercury(II) with a surface-enhanced Raman scattering sensor based on functionalized gold nanoparticles. *Materials Research Express*, *4*(5), 055017. https://doi.org/10.1088/2053-1591/aa6c7b

Zheng, S., Li, D., Fodjo, E. K., & Deng, W. (2020). Colorimetric/fluorescent/SERS triple-channel sensing of Cu2+ in real systems based on chelation-triggered self-aggregation. *Chemical Engineering Journal*, *399*. https://doi.org/10.1016/j.cej.2020.125840

Zhou, Q., Zhang, J., Fu, J., Shi, J., & Jiang, G. (2008). Biomonitoring: An appealing tool for assessment of metal pollution in the aquatic ecosystem. *Analytica Chimica Acta*, *606*(2), 135–150. https://doi.org/10.1016/j.aca.2007.11.018

Zhou, W., Saran, R., & Liu, J. (2017). Metal sensing by DNA. *Chemical Reviews*, *117*(12), 8272–8325. https://doi.org/10.1021/acs.chemrev.7b00063